Published in final edited form as:

J Control Release. 2017 September 10; 261: 62–86. doi:10.1016/j.jconrel.2017.05.033.

Multifunctional nanodiamonds in regenerative medicine: recent advances and future directions

Jonathan Whitlow[1], **Settimio Pacelli**[1], and **Arghya Paul**[1,2,*]

[1]BioIntel Research Laboratory, Department of Chemical and Petroleum Engineering, School of Engineering, University of Kansas, Lawrence, KS 66045, USA

[2]Bioengineering Graduate Program, University of Kansas, Lawrence, KS, USA

Abstract

With recent advances in the field of nanomedicine, many new strategies have emerged for diagnosing and treating diseases. At the forefront of this multidisciplinary research, carbon nanomaterials have demonstrated unprecedented potential for a variety of regenerative medicine applications including novel drug delivery platforms that facilitate the localized and sustained release of therapeutics. Nanodiamonds (NDs) are a unique class of carbon nanoparticles that are gaining increasing attention for their biocompatibility, highly functional surfaces, optical properties, and robust physical properties. Their remarkable properties have established NDs as an invaluable regenerative medicine platform, with a broad range of clinically relevant applications ranging from targeted delivery systems for insoluble drugs, bioactive substrates for stem cells, and fluorescent probes for long-term tracking of cells and biomolecules *in vitro* and *in vivo*. This review introduces the synthesis techniques and the various routes of surface functionalization that allow for precise control over the properties of NDs. It also provides an in-depth overview of the current progress made towards the use of NDs in the fields of drug delivery, tissue engineering, and bioimaging. Their future outlook in regenerative medicine including the current clinical significance of NDs, as well as the challenges that must be overcome to successfully translate the reviewed technologies from research platforms to clinical therapies will also be discussed.

Graphical Abstract

*Correspondence: Arghya Paul, arghyapaul@ku.edu.

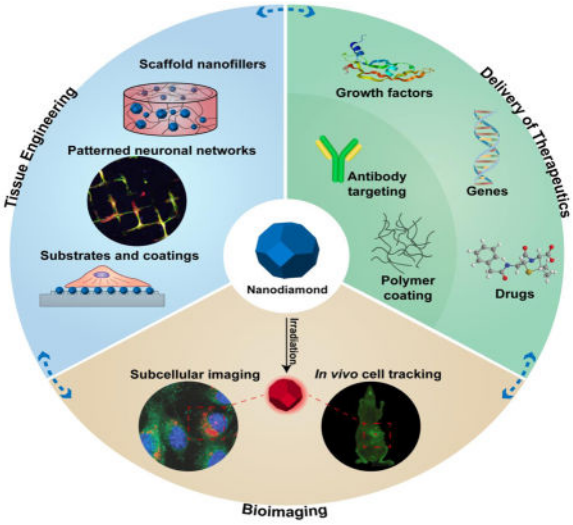

1. Introduction

Nanodiamonds (NDs) are an emerging class of carbon nanomaterials which possess a unique set of chemical, physical, and biological properties essential for the design of innovative therapies in the fields of drug delivery, tissue engineering, and bioimaging. Over the last two decades, several synthesis techniques have been optimized to enable the fabrication of NDs with a defined size, morphology, and homogeneous surface chemistry. The discovery of improved purification methods and surface modification strategies have also facilitated the production of NDs with precise and customizable features [1]. The inherent physical and chemical properties of NDs make them suitable candidates as delivery agents for many therapeutic molecules. For instance, their high surface area to volume ratio and tunable surface chemistry enables the high loading capacity of small molecules containing amine groups or other polar moieties by physical adsorption. Following this reversible loading technique, poorly soluble drugs such as anthracyclines can be non-covalently linked to NDs that possess hydroxyl or carboxyl groups on their surfaces [2]. This facile loading process is efficient and does not require any chemical modification. Moreover, NDs have demonstrated to improve the therapeutic efficacy of many chemotherapeutic agents by increasing their dispersivity in water, facilitating their sustained release, shielding the drug from inactivation, and bypassing the mechanisms of chemoresistance [3, 4]. These significant improvements in the delivery of chemotherapeutic agents have inspired researchers to study NDs for the sustained release of other therapeutic molecules, such as growth factors, peptides, and genes [5]. In fact, NDs are rapidly internalized by cells but do not readily undergo exocytosis, which localizes the release of bioactive molecules within the cell for an enhanced therapeutic effect [6]. Proteins such as insulin and bone morphogenetic protein-2 (BMP-2) have been adsorbed onto carboxylated NDs and administered both *in vitro* and *in vivo* to achieve a pH-dependent sustained release [7, 8]. Additionally, the presence of polar groups on the surface of NDs enables the nanoparticle to adsorb positively charge polymers such as polyethyleneimine or polylysine, which serve as intermediate cationic layers to promote the adsorption of DNA and RNA [9].

Meanwhile, NDs have also been evaluated as a nanofiller for reinforcing the mechanical properties of composite scaffolds to rival that of human tissue [10, 11]. By establishing covalent or ionic bonds with the polymeric chains during the scaffold preparation, NDs can be used to modulate the mechanical properties of polymeric networks to mimic the structure of both soft and hard tissues of the human body [12]. NDs have also found applications as bioactive coatings to improve the tribological properties and reduce the mechanical wear of orthopedic implants [13]. The high biocompatibility of NDs in comparison with other carbon nanomaterials such as graphene oxide or single and multi-walled carbon nanotubes represents a significant advantage for NDs and suggests the high probability for the clinical translation of ND-based treatments [14].

Finally, the optical properties of fluorescent NDs (FNDs) have sparked a great interest among researchers for the use of these nanoparticles as imaging probes. NDs can be modified to introduce nitrogen vacancies in their inner diamond core that emit a highly stable fluorescence. These nitrogen vacancies, which emit a bright fluorescence in the far-red spectrum, are located within the sp^3 carbon lattice structure allowing for surface modification without disrupting the vacancy centers or reducing the fluorescence intensity. FNDs possess high photostability, high quantum efficiency and longer fluorescent lifetimes when compared to other organic fluorophores used for cellular imaging [15].

In this review, we will highlight the strategies available for the synthesis and the chemical modification of NDs' surface with particular attention on how they may affect their biocompatibility. This section will be followed by an overview of the possible applications of NDs in the field of drug delivery, tissue engineering and bioimaging describing the current challenges yet to overcome (Figure 1A). Finally, particular emphasis will be given to the design of multidisciplinary approaches in which NDs can be employed as a nanocarrier for drugs or genes while functioning as fluorescent probes or as nanofilling agents in bone tissue scaffolds. The ability of NDs to present multimodal functionality is what makes them truly unique from other nanomaterials, and thus, NDs have a very bright future as both a research tool and as a clinical theranostic platform.

2. Synthesis and functionalization of NDs

NDs were first discovered in 1963 by researchers in the USSR who were performing detonation tests with carbon-based explosives. Upon detonating a mixture of 2,4,6-trinitrotoluene (TNT) and 1,3,5-trinitroperhydro-1,3,5-triazine (RDX) in a blast chamber, the researchers found that the soot contained 4–5 nanometer diamond particles accompanied by graphite and other non-diamond carbon particles [16]. Despite their early discovery, the properties of these nanoparticles were not researched for biomedical applications until the beginning of the 21^{st} century. NDs can be produced in different sizes such as nanocrystalline particles (1–150 nm) or ultra-nanocrystalline particles (2–10 nm). The core of the nanoparticle is a sp^3 hybridized carbon lattice that is surrounded by sp^2 hybridized carbon and various oxygenated functional groups [17].

The size of the diamond core, the distribution of the sp^2 regions in the outer shell, as well as the diversity of reactive functional groups on the NDs' surface, are substantially influenced

by the route of synthesis and the composition of the reactants. In addition, the physicochemical properties can also be affected by the purification steps, which are necessary for removing undesired impurities that are introduced during synthesis. An overview of these fundamental aspects will be examined with an emphasis on strategies aimed to homogenize the NDs' surface chemistry, which is an essential requirement for their potential application in biomedical research.

2.1. Synthesis techniques

Several methods are available for the fabrication of NDs including detonation synthesis, chemical vapor deposition (CVD), high-pressure high-temperature (HPHT), and laser techniques. Each one of these technologies has a profound impact on the size and surface properties of the obtained NDs. The choice of a particular strategy can also influence the degree of agglomeration and level of purity of the nanoparticles, which are both aspects that need to be accurately tested when prior to further use of NDs in drug delivery, tissue engineering, or bioimaging applications. For this reason, signficant effort has been made to fabricate NDs with controllable size and homogeneous surface features to reduce the level of variability associated with their fabrication. Both the advantages and limitations of each synthesis approach will be discussed in the following sections with particular attention to the emerging solutions designed to achieve a precise control over the NDs' properties.

2.1.1 Detonation synthesis—Detonation nanodiamonds (DNDs) are formed by high temperature and pressure reactions resulting from the detonation of mixtures of carbon explosives such as TNT and RDX or 2,4,6-triamino-1,3,5- trinitrobenzene (TATB) in oxygen-deficient reaction chambers. The combustion reaction produces extreme operating conditions at which sp^3 diamond becomes the thermodynamically favored bulk phase of carbon; shortly after detonation (<100 ns) the diffusive coagulation of clustered carbon atoms results in the formation of this bulk sp^3 phase [18]. As the soot of detonation is cooled at a controlled rate in either a gas or liquid phase medium, sp^2 hybridized carbon and other impurities are deposited in layers surrounding the diamond lattice. These partially graphitized diamond crystallites, known as DNDs, have an average diameter of 4–5 nm and possess a truncated octahedral morphology (Figure 2A) [19]. Overall, the detonation synthesis is a process associated with a poor degree of control over the NDs' purity. This issue is due to the presence of non-carbon species in the explosive reactants, which introduces in the lattice and the outer shell of DNDs a wide diversity of impurities such as nitrogen, metals, and some carbides [20].

For this reason, several purification steps are necessary including magnetic separation, filtration, and oxidation by washing with strong acids like sulfuric acid and nitric acid. Removal of the sp^2 carbon shell can also be achieved by oxidizing NDs in air with ozone at high temperature without the utilization of any corrosive liquid [21]. These steps are expensive and increase the final cost of fabrication significantly. Another drawback of the detonation approach is the limited control over the surface chemistry along with the considerable variability in surface chemistry from batch to batch. DNDs typically present negatively charged function groups on their surfaces in the form of carbonyl, hydroxyl, epoxy or carboxyl groups. Additionally, the composition of functional groups on the surface

may also vary according to the process of cooling after the explosion which can be obtained in a dry chamber with an inert gas or in wet condition using water.

Finally, another limitation of this technique is that the resulting DNDs have a strong affinity to form aggregates in aqueous suspension, and these clustered networks can form up to 200 nm in diameter [22]. DNDs tend to aggregate due to the high density of reactive groups on the surface and the small size. The process of aggregation can be caused by the formation of covalent bonds among the particles or other types of weak interactions including hydrogen bonds, van der Waals forces and π-π stacking due to the presence of graphitic regions. Therefore, in addition to removing metallic impurities, DNDs require a further step of purification after their synthesis to increase their colloidal stability. These strategies will be further analyzed in the following section.

2.1.2 Deagglomeration strategies of DNDs—To effectively overcome the problem of agglomeration and create stable suspensions after detonation synthesis, several factors can be modulated such as the surface charge, the steric hindrance and the size distribution of DNDs. Each one of these factors can impact the stability of DNDs once suspended in aqueous medium and determine their suitability for biomedical applications. For instance, it is well established that highly charged nanoparticles do not aggregate due to electrostatic repulsion. Based on this concept, a straightforward approach to modifying the surface charge of DNDs consists in the addition of electrolytes or ionic surfactants in solutions that can increase the absolute value of the zeta potential, which is a measure of the electric potential between the solvent shell around the ND and the bulk medium [23]. Similarly, DNDs with high positive zeta potential can be obtained by hydrogen annealing treatment at a temperature above 800° C, which enables the formation of hydrogenated DNDs that present high colloidal stability [24].

Moreover, the surface can be modified with synthetic polymers to increase the DNDs colloidal stability by creating a shell that can generate enough steric hindrance to reducing agglomeration among the nanoparticles [25]. Polyethylene glycol (PEG) along with its methacrylate derivatives and hyperbranched polyglycerol (PG) are typical examples of polymers investigated to form hydrophilic shells on the surface of DNDs which have been successfully used to increase their stability in aqueous solution [26, 27].

Aside from the surface properties, the particle size also affects the tendency for NDs to aggregate. Smaller particles display higher colloidal stability, while larger NDs exhibit a much lower colloidal stability. As discussed in the previous section, the conditions employed during detonation synthesis do not allow control over the size of the produced DNDs and a variety of strategies have been designed to decrease the size of DNDs after synthesis to generate nanoparticles with narrower size distributions. These techniques include milling with silica or zirconia microbeads, which have been proven successful in reducing the nanoparticle size of DNDs to dimensions below 10 nm and in increasing their dispersivity [28, 29]. However, these methods, which involve the use of mechanical energy to disaggregate ND clusters, present a series of limitations such as the possible contamination of NDs with impurities derived from the bead material. For instance, ZrO_2 impurities that result from milling with zirconium beads are difficult to remove and require further

treatment with strong acids or bases after milling. To overcome this issue, the process of milling can instead be conducted with crystalline media such as sucrose or sodium chloride without the utilization of any beads made of zirconia or silica. In this case, the milling media can be removed completely by washing DNDs with water although metal impurities derived from the mill may still require removal in further purification steps [30]. Similarly, an alternative strategy to reduce the size of DNDs is the use of ultrasound in the presence of salts such as NaCl, KCl, or CH_3COONa, which can be eliminated after the process of segregation. The presence of salts can also significantly improve the colloidal stability by increasing the absolute value of the zeta potential of DNDs [31].

2.1.3 Alternative synthesis approaches to detonation—In addition to detonation, refined methods of ND synthesis have also emerged to produce NDs with improved features in terms of size distribution and homogeneous surface chemistry. For instance, chemical vapor deposition (CVD) consists of the injection of methane and hydrogen gas in a plasma reactor [32]. CVD is commonly utilized to form thin ND films with thicknesses varying from 5 to 100 nm (Figure 2B) [33, 34]. Since hydrogen gas is used to direct the deposition of carbon, the resulting NDs are hydrogen-terminated and do not contain many of the structural impurities found in DNDs. To obtain films of lower thickness (3–5 nm), hydrogen can be replaced with argon. This technique is commonly chosen for the formation of ultra-nanocrystalline diamond coatings on metallic biomedical implants. NDs films exhibit high surface roughness, dense structure and low cytotoxicity with superior performance compared to other types of material such as platinum or quartz [35]. Additionally, NDs films possess excellent mechanical properties such as high resistance to fracture, high Young's modulus, and low friction coefficients. A more in-depth discussion about the applications of NDs film can be found in another excellent review [36].

An alternative technique for the production of NDs is high-pressure and high-temperature (HPHT) synthesis that transforms a graphitic precursor into single phase NDs that are free of sp^2 defects [37]. Additionally, the temperature and pressure can both be adjusted during operation to precisely control the size and morphology of NDs. HPHT synthesis is most commonly complemented with bead-assisted sonic disintegration or high-pressure milling to reduce the nanoparticle size. HPHT synthesis produces NDs with a discernible euhedral structure. Coupled with bead-assisted milling techniques to enhance dispersivity, HPHT NDs display sharply faceted outer surfaces. HPHT synthesis is often favored over detonation synthesis because HPHT NDs are formed in a more uniform size and contain fewer lattice defects than DNDs. Moreover, NDs produced by the HPHT technique tend to form fewer aggregates when compared to DNDs, and to increase their colloidal stability, the surface can be modified with amino-silica or other types of polymer coatings (Figure 2C). HPHT synthesis has been used to create NDs as small as 1.1 nm, the smallest artificial NDs ever recorded [38]. This process of synthesis is also suitable for the fabrication of NDs with a high content of nitrogen (100 – 300 ppm) in their diamond core which can be useful for the manufacture of fluorescent NDs. For example, HPHT NDs can be treated with high energy irradiation followed by thermal annealing to create carbon-nitrogen vacancies that are responsible for their fluorescent properties. One of the drawbacks associated with the HPHT

approach is the high production cost, which is relatively higher in comparison to detonation synthesis and limits the mass preparation of NDs using this strategy.

2.1.4. Laser-based strategies to fabricate NDs—Aside from the aforementioned strategies, NDs can be generated by laser ablation in liquid (PLAL) techniques, which is more environmental friendly and less hazardous compared to detonation synthesis. These technologies have been so far investigated for the production of NDs in the laboratory, although the recent advancements in this field have allowed the design of less expensive methods that can potentially be implemented on an industrial scale.

PLAL synthesis, which offers precise control over particle size during synthesis, is performed by focusing a laser onto a carbon-based target material surface immersed in water or acetone. During the process, small amounts of target material evaporate and remain entrapped in microbubble. The carbonaceous material trapped inside the bubble will experience a high pressure and temperature which is responsible for the formation of the NDs. This synthesis technique, though much more costly than detonation synthesis, yields NDs with high carbon content and minimal metallic impurities [43].

An alternative approach is defined as light hydro-dynamic pulse (LHDP) synthesis. In this case, the radiation beam is focused in a transparent liquid at a certain selected distance from the target composite material, which is made of commercially available carbon soot and hydrocarbons. The formation of the NDs is mainly due to the impact of the acoustic shock wave generated by the laser on the surface of the composite material. The obtained NDs can be purified and isolated from the non-diamond soot using organic solvents, and then washed with water and dried. The LHDP synthesis enables a precise control over the size (4–5 nm) and several parameters can be adjusted to achieve this degree of accuracy. For instace, the distance of the laser beam from the target surface, the energy flux, the composition of the carbon soot, and the width or shape of the laser pulse are all parameters that can influence the size [44]. Finally, in a more recent study, NDs with a size less than 5 nm were successfully produced directly from ethanol without the use of any carbon soot by using femtosecond laser irradiation (Figure 4D). This approach could be an alternative to producing NDs with defined size simply by varying the intensity of the laser [45].

A summary of the advantages and limitations of each synthesis technique described so far can be found in Table 1.

2.2. Chemical strategies for surface homogenization

After synthesis, chemical treatment of NDs is often necessary to create homogenized reactive surfaces that enable further surface modifications. The initial functional groups present on the surface of an ND following the formation of the nanoparticle varies based upon the synthesis and purification methods that are chosen. Since the ratio of polar to non-polar functional groups on the surface of NDs defines several important properties, such as their hydrophobicity or hydrophilicity, it is essential to establish reproducible methods to ensure uniformity or homogeneity of their surface chemistry. Some synthesis techniques, such as hydrogen-assisted CVD, can be used to produce NDs with homogenous hydrogen-terminated surfaces. On the contrary, other methods such as detonation synthesis introduce a

highly diverse surface chemistry to NDs, with functional groups including hydroxyl, carbonyl, ether and carboxyl groups. These groups are commonly generated on the surface of DNDs during the step of rapid cooling using water or through the step of oxidation with strong acids. To further chemically modify this type of NDs it is then required a process aimed to ensure a similar functionality throughout the entire surface. Among the possible alternatives, carboxylation, hydroxylation or hydrogenation are the routes most commonly investigated.

Carboxylation can be carried out using both liquid and vapor oxidation reactions which help purify DNDs by oxidizing the non-diamond carbon and terminating the surface with carboxyl (-COOH) groups. Acid oxidation with sulfuric acid and nitric acid or with sulfuric acid and hydrogen peroxide are both effective methods of aqueous COOH homogenization that remove non-diamond carbon and other metallic impurities from the detonation soot. Researchers have developed several methods for oxidizing NDs that do not require acid treatments, such as the oxidation of detonation soot with supercritical H_2O and hydrogen peroxide [46, 47]. Additional techniques for the vapor phase carboxylation of NDs include oxidation of the detonation powder with air at high temperatures (350–450°C) or oxidation in ozone at lower temperatures (150–200°C) [48, 49]. These environmentally-friendly vapor phase oxidation methods can be controlled to remove sp^2 carbon impurities with precision.

Hydroxylation is another surface homogenization pathway that terminates the surface of NDs with hydroxyl (-OH) groups by oxidative, reductive, or even mechanical techniques. The selection of the correct mechanism for successful hydroxylation depends on the preliminary surface composition of the ND. For example, hydroxylation of NDs containing amorphous carbon impurities is most effective when conducted by reaction with Fenton's reagent, a mixture of $FeSO_4$ and H_2O_2. Fenton's reagent oxidizes non-diamond impurities and produces OH radicals which densely terminate the ND surface [50, 51]. Alternatively, DNDs can be treated with borane, a reductive hydride, which can reduce carbonyl groups with the exception of lactones and esters [52]. Reduction with $LiAlH_4$, on the other hand, can reduce any type of carbonyl group, and therefore is a highly efficient method for producing OH-terminated NDs [53, 54]. DNDs can also be hydroxylated by mechanical techniques, such as the sonication and milling of detonation soot in water, which causes a radical reaction that facilitates the hydroxyl surface termination [55]. Hydroxylated NDs are hydrophilic, more stable in suspension than unmodified DNDs, and can take part in further covalent and non-covalent modifications.

DNDs can also be hydrogenated by treating the detonation soot with elemental hydrogen at temperatures as high as 900°C. However, small NDs (<100 nm) cannot withstand such high temperature and therefore they require hydrogenation at lower temperatures. This change in this physical parameter can limit the degree of hydrogenation of the surface and can also result in the formation of hydroxyl terminations. As a more efficient alternative, hydrogen plasma is often used to hydrogenate the surface of NDs. Loh *et al.* reported the efficient reduction of oxidized DNDs by exposing the nanoparticles to hydrogen plasma [56]. Hydrogen-terminated NDs are hydrophobic, stable in suspension, and display *p*-type conductivity which can facilitate further surface modifications [57, 58].

Aside from these three major routes described so far, other strategies have also been explored to modulate the reactivity of the DNDs' surface. A possible alternative is the fluorination of the surface using a gas mixture of $F_{2//}H_2$ at elevated temperatures or using plasma treatment [59]. The presence of fluorine atoms enables for further substitutions with alkaline reagents such as amines and Grignard's reagents. Other halogens such as chlorine have also been introduced by plasma treatment of NDs with Cl_2 or CCl_4 [60]. However, chlorinated NDs have been reported to be extremely reactive in the presence of humidity and oxygen, and the rapid substitution of the halogen with hydroxyl groups upon direct contact with air may limit their long-term stability.

Finally, another approach to guarantee the uniformity of the surface is the removal of all the functional groups. This result can be obtained through thermal treatment. After this process, all the heteroatoms are removed from the surface, and it becomes evident the conversion of DNDs into "Bucky diamonds" which display a multilayer of sp^2 carbon around the diamond core [61]. The temperature and the size of the DND are crucial parameters in determining the extent of graphitization which can in certain conditions involve the entire core of the DNDs. In this case, it is instead possible the formation of carbon onions which is made of a multi-shell of graphitic layers. Carbon onions do not behave like DNDs and display completely different reactivity.

2.3. Covalent conjugation strategies

Once the correct functionality has been homogeneously introduced on the surface of NDs further chemical modifications are possible to covalently link biomolecules, drugs, antibodies or fluorescent probes. The type of bond and its stability in an aqueous environment or the presence of enzymes are critical parameters that have to be considered for a successful therapy. For instance, amide bonds offer greater stability than ester groups, and for this reason, they are more indicated for the immobilization of enzymes on the surface of NDs. On the contrary, groups that are more inclined to hydrolysis such as anhydrides or carbonates will be more useful for the design of drug delivery strategies where the therapeutic molecule needs to delivered and released from the surface of the NDs.

NDs represent a platform which enables a great variety of chemical modifications based on the functional groups introduced with a previous step of chemical homogenization. For example, purified COOH-terminated NDs can be used to generate ester or amide bonds although a previous activation of the carboxyl group is required. Specifically, thionyl chloride ($SOCl_2$) is the preferable method of carboxyl activation which leads to the formation of a more reactive acyl chloride derivate [62]. Alternative ways of activation consist of the use of carbodiimides or standard reagents employed in peptide chemistry. Once activated, carboxyl groups can react with alcohols or amines to form esters or amide groups respectively. Esters bonds are more prone to hydrolysis in an aqueous environment than amide groups although the latter can be cleaved by protease enzymes. Amide bonds are the best choice to achieve immobilization of proteins onto the surface of NDs due to their inherent chemical stability.

Another possibility to form amide bonds is when the NDs are displaying amino groups. The amino group is nucleophilic and can react with molecules carrying activated carboxylic

groups or with anhydrides. Direct amination of NDs has been possible on nanodiamonds films using plasma treatment with ammonia [63]. However, common strategies for introducing amino groups on NDs rely on the addition of a spacer which carries the amino functionality. For instance, hydroxylated NDs can be modified with aminated aromatic groups or aminated silanes [64]. Alternatively, fluorinated NDs can also be used to generate amino functionalized NDs by substitution of the halogen with NH_3 at high temperature.

Hydroxyl-terminated NDs can also represent a useful starting point for carrying out a diversity of chemical conjugations involving biomolecules. One of the available options is the substitution reaction with alkyl chlorides in the presence of NaH to create stable ether bonds-Alcohols can also react with acyl chlorides to form esters although they may get hydrolyzed once introduced in polar solvents. For this reason, esterified-NDs need to be dispersed in apolar solvent to preserve their integrity.

Similarly, the bond O-Si obtained from the reaction of hydroxyl groups on the surface of NDs and trialkoxysilanes is not stable at low pH and often the presence of adjacent hydroxyl group can also lead to intramolecular condensation. To avoid this problem, it is possible to choose mono or dialkoxysilanes. The Si-OR bond is a reactive center that can be subjected to nucleophilic substitution allowing for the conjugation of proteins [65].

An interesting reaction which can be followed to conjugate proteins is the use of benzoquinone molecules which readily react with hydroxyl groups through Michael addition. The intermediate ND-benzoquinone complex can be used to covalently link proteins which will be able to attach to the benzoquinone molecules using side amino groups of lysines. Following this method, Purtov *et al.* [66], have successfully conjugated simultaneously bovine serum albumin and the immunoglobulin protein G IgG on hydroxylated NDs modified with benzoquinone molecules.

Hydroxyl groups on the NDs surface can also react with epoxy groups to form hyperbranched polymer coatings. For instance, this strategy has been used to coat the surface of NDs with polymers such as polyglycerol (PG) which can be formed by ring opening polymerization directly on the surface of NDs in the presence of the monomer glycidol. Furthermore, this polymer coating can be modified by converting the terminal hydroxyl groups of PG into azide (N_3) groups which can serve as a linking point for click chemistry reactions with a polypeptide carrying alkyne groups in the side chain [67].

Aside from covalent strategies carboxyl and hydroxyl-terminated NDs are also able to create hydrogen and dipole ion physical bonds with polymeric chains or large proteins. DNDs which are rich on oxygenated functionalities such as carbonyl, hydroxyl, and ether groups have been used successfully for the adsorption of several proteins including lysozyme and cytochrome c simply by physical adsorption [68]. Similarly, carboxylic functions on the NDs' surface can establish electrostatic interactions with a variety of positively charged polymers such as polylysine, polyaniline and polyarginine forming polymeric coating that can be useful for the targeting of drugs and genes. Specific examples on this topic can be found in another excellent review [69].

Finally, hydrogenated NDs present *p*-conductivity as well as ease electron transfer ability which are both reasons of their high reactivity. In fact, hydrogen-terminated NDs can be chosen for covalent conjugation allowing the formation of new C-C covalent bonds with the lattice of the NDs. These bonds are chemically stable, and they are not readily cleaved by enzymes like in the case of amide groups. Specifically, one of the most investigated reaction is the one involving photochemical grafting of alkenes. The reaction consists in the UV-mediated photorejection of electrons from the surface of H-terminated NDs. An alkene in the liquid phase can accept the electron from the surface forming a radical anion which becomes responsible for the extraction of a hydrogen from the surface leaving a carbon radical. This is the center of grafting which will start the polymerization [57]. NDs hydrogen-terminated due to their ability to donate electrons can also react with aryldiazonium salts which can contain additional functional groups such as amines or hydroxyl groups for further substitutions. Similarly to hydrogenated surfaces, NDs displaying a shell of graphitic carbon can participate in the same coupling reaction with aryldiazonium salts. Moreover, the shell of sp^2 can be used to carry out Diels-Alder reactions with dienes forming new C-C bonds. In fact, the graphitic part of the surface in bucky NDs can act like a dienophile and can undergo a [4+2] cyclic addition. A summary of all the possible chemical modification detailed in this section are reported (Figure 3).

It is important to underline that every modification described can have a profound impact not only on the reactivity of the surface but also on the general biocompatibility of the NDs. Due to the importance of this biological aspect, a detailed discussion will be presented in the next section.

2.4. Biocompatibility of NDs

NDs present a lower profile of toxicity when compared to other carbon-based nanomaterial such as graphene oxide or carbon nanotubes [70]. This great advantage combined with their high cellular uptake make them the ideal candidate for the design of novel therapies for drug delivery and tissue engineering. However, as for other types of carbon-based materials, several factors must be considered and thoroughly investigated prior to their transition into the clinic. These include the possible toxicity induced by their physical and chemical properties. For instance, the surface chemistry or the size of NDs are major variables that can modulate the level of oxidative stress or alter the expression of apoptotic genes. Finally, aside from their inherent features, another aspect that should be considered is their biodistribution and their site of accumulation once administered *in vivo*. All these critical points have been the object of intensive study in the last decade and will be highlighted in the following sections.

2.4.1 Main factors influencing DNDs cytotoxicity—As previously discussed, the type of synthesis can modulate the size distribution, the morphology, the degree of aggregation, the surface functional groups and the level of impurities of the obtained NDs. Each one of these factors can induce cytotoxicity, which may vary according to the concentration used, the time of exposure and the cell line tested.

Among all the strategies for the production of NDs, detonation synthesis produces NDs with the highest level of toxicity mainly due to the introduction of impurities including carbon allotropes, carbon soot, oxides carbides and other metals. These impurities can induce increase oxidative stress and alteration in the activity of antioxidant enzymes. For instance, upon exposure to non-purified DNDs, a decrease in the enzymatic levels of superoxide dismutase, glutathione reductase, and glutathione S-transferase are generally observed in human umbilical vein endothelial cells (HUVECs) [71–73] Moreover, DNDs without any step of purification have been reported to reduce angiogenesis. Upon incubation of DNDs with chicken embryos, ND exposure caused a downregulation of bFGF expression, which led to a decrease in the angiogenic activity. Histological analysis determined that DNDs exposure resulted in a decline in both the density and length of vessels in the embryos, though no other cytotoxic or detrimental effects were observed [74]. Similarly, in a comparative study of different carbon-based nanomaterial DNDs produced the highest antiangiogenic effect in ovo chicken embryo chorioallantoic membranes (CAM) and this effect was explained by the reduction induced by DNDs on the levels of pro-angiogenic growth factor receptors [75]. Aside from impurities, the size of DNDs is generally another parameter that can induce increase cytotoxicity. For instance, Solarska *et al.* have investigated the apoptotic effect on HUVECs of DNDs in comparison with another type of NDs produced by CVD technique. The DNDs showed the highest apoptotic effect on HUVECs compared to the other systems. The authors attributed this trend mainly to the smaller size of the DNDs, and similarly to other reports, to the presence on the surface of reactive functional groups capable of generating radical oxygen species. However, the morphology and the structure of the different nanodiamonds investigated did not seem to play a major role in promoting apoptosis in HUVECs [73]. Similar findings were also observed in other cell lines, such as rat osteosarcoma cells and rat primary mesenchymal stem cells, where the higher level of cytotoxicity was strictly dependent on the size and level of impurities of DNDs. On the contrary, DNDs that were purified and were larger in size did not elicit any toxic response in the same cell lines [76].

2.4.2 Influence of surface chemistry on the NDs cytotoxicity—As reported in section 2.2, NDs are chemically modified to introduce a specific functionality on their surface to reduce the level of heterogeneity commonly obtained after detonation synthesis. Whether this change in the surface chemical composition may affect, their biocompatibility has been the main topic of investigation for the last decade of research. The results of several studies in this area are controversial, and a definitive conclusion cannot be drawn. In fact, each single study needs to be evaluated separately based on multiple factors including the type of functional group introduced, the size of NDs, the cell line tested and the concentration of NDs tested. Having in mind these criteria, we have summarized the main findings by highlighting the possible cytotoxic effect induced by the surface modification of NDs For example, Paget *et al.* observed that NDs, carrying carboxylic groups (ND-COOH) with diameters of 20 nm and 100 nm and concentrations as high as 250 μg/mL, caused neither genotoxic nor cytotoxic effects in cultures of six different types of human cell lines [77]. On the contrary, a different study reported the genotoxic effects of ND-COOH on embryonic stem cells (ESCs), which was higher when compared to DNDs [78]. Additionally, ND-COOH induced alterations in the cell cycle of ESCs affecting their ability

to differentiate, and this effect was not observed when ESCs were exposed to DNDs. Marcon *et al.* compared the toxicity of ND-OH, ND-NH_2, and ND-COOH both *in vitro* in embryonic kidney cells (HEK) and *in vivo* in *Xenopus* embryos [79]. These experiments confirmed a dose-dependent trend of cytotoxicity both *in vitro* and *in vivo* for NDs of all three surface chemistries, although none of the types of NDs in this investigation were as cytotoxic as gold nanoparticles. When administered to *Xenopus* embryos, ND-OH and ND-NH_2 had no effects on embryogenesis whereas ND-COOH affected the gastrulation and neurulation phases of development and caused phenotypical defects at concentrations up to 200 μg/mL. However, the observed malformations during embryogenesis were likely caused by physical obstruction upon the aggregation of NDs and not due to ROS production [79].

An in-depth investigation of the possible interactions between cells and ion-functionalized NDs was reported by Zhu *et al.* to study the use of NDs for delivering ions to controllably induce ROS production and cell apoptosis [80]. The group reported that the highly adsorptive surfaces of NDs and their rapid cellular internalization enabled the controlled release of cytotoxic divalent ions within cells while inhibiting or shielding all of the toxic effects of the ions prior to desorption. Ions from metals such as copper, chromium, and nickel were adsorbed to NDs, and their release occurred by pH-triggered desorption, which resulted in the formation of ROS inside cells. This evidence of nanoparticle-mediated ion penetration of the cellular membrane sheds new light on ND toxicology and offers a unique perspective on nanomaterial cytotoxicity.

Finally, the biocompatibility of NDs can also be affected by the presence of surface coatings which are commonly applied to prevent their aggregation in suspension. Aggregation is a significant roadblock for the use of NDs in many biomedical applications, so polymers or small molecules are frequently conjugated to NDs to solve this issue and increase the long-term stability of ND complexes in suspension. Several parameters including the molecular weight and the charge composition of the polymer coating selected can significantly affect their biocompatibility.

For instance, polyaniline (PANI) is a commonly used conductive polymer, and by oxidative polymerization of aniline in the presence of NDs, ND-PANI complexes can be formed exhibiting increased dispersivity than DNDs.[81] Similarly to previously discussed types of functionalized NDs, ND-PANI displayed a dose-dependent trend of cytotoxicity when incubated with human embryonic kidney (HEK-293) cells *in vitro*. While lower concentrations (1 μg/mL) of ND-PANI had no adverse effects on the cells, higher concentrations (10 μg/mL) were reported to be cytotoxic and warrant further study before use. Furthermore, octadecylamine (ODA) is another molecule with many applications in nanomedicine. ODA can be covalently linked to NDs to form ND-ODA, which exhibit high dispersivity in non-polar solvents. Zhang *et al.* have reported that ND-ODA, as well as ND-ODA-PLLA nanocomposites, are non-cytotoxic when exposed to 7F2 osteoblasts *in vitro* at concentrations as high as 100 μg/mL [82]. A summary relative to the influence of the surface modification on the NDs' cytotoxicity in different cell lines is reported in Table 2.

2.4.3 Cellular uptake pathways and biodistribution of NDs *in vivo*—NDs have attracted significant attention in biomedical research due to their biocompatibility and rapid

transmembrane transport which is favorable for the design of efficient delivery strategies for drugs, proteins, and genetic material [89].

The primary cellular uptake pathway for NDs has been confirmed in a broad range of cancer and stem cell lines to be clathrin-mediated endocytosis [83, 90–92]. However, NDs have a strong affinity to aggregate, and in this form, the cellular uptake most commonly occurs by macropinocytosis, or plasma membrane ruffling [83, 92]. Upon internalization, small NDs (< 10 nm) localize in the cytoplasm, and larger NDs remain in vesicles. Notably, NDs have never been observed to enter a cell's nucleus [83, 90, 92]. In most cell lines, once NDs have been internalized they exhibit an inherent resistance to exocytosis, but some types of cells such as adipocytes have been reported to facilitate the efflux of NDs by exocytosis [91].

Moreover, once internalized NDs do not affect any phase of the cell cycle. For instance, it was found that the cell cycles of adenocarcinoma cell lines and embryonic fibroblasts were not affected by FND-labeling in cell cultures up to 10 days, and additionally, the differentiation of the embryonic fibroblasts was not altered in any manner by the FNDs [83]. Upon telophase of the cell cycle, the FNDs migrate to the cytoplasm of each daughter cell without disrupting any mitotic activities. These qualities were all observed while the FNDs were tracked at a single-cell resolution *in vitro* for over a week.

Aside from studying the main pathways of internalization by cells and their fate upon internalization, NDs have also been evaluated for their biodistribution after administration *in vivo* in animal models using several routes of administration. For instance, Yuan *et al.* reported that 28 days after administering DNDs to mice by bolus injection, 68% of the loading dose was still present with a majority of the NDs localized to the liver and lungs [93]. Alternative routes of administration have also been studied such as the intratracheal instillation of DNDs in mice [94]. Three days after exposure, DNDs had accumulated primarily within the lungs; however, DNDs were found to migrate across the air-blood barrier of the lungs into the bloodstream, and all vital organs such as the heart, liver, and kidney were all exposed to DNDs. While system exposure by this route of administration is a concern, cytotoxicity occurs only when NDs are present in very high doses. Similarly, in another study the pulmonary toxicity in mice was investigated after intratracheal instillation administration of NDs having 4 nm size at the concentration of 1 mg/Kg. The NDs did not cause any significant toxic effect in lungs and were engulfed by macrophages and cleared in the pharynx with the assistance of the escalator/mucociliary system [95]. Biodistribution has also been studying in non-human primates in a six-month study where NDs have been administered in monthly bolus injections. NDs did not affect the organ functions at moderate or high concentrations 15 mg/kg and 25 mg/kg, respectively. Analysis of complete blood counts, serum chemistry markers, and urinalysis concluded no significant differences in organ function or serum composition between non-human primates that were treated with DNDs and the control group which was left untreated [96].

3. Delivery of therapeutics

Recent advancements in nanotechnology have led to the development of nanoparticle carriers that significantly enhance the therapeutic activity of drugs, genes, and other

biomolecules while reducing or preventing harmful side effects. At the forefront of this research is the study of nanodiamonds, which can not only be utilized to load and release bioactive cargo but at the same time can be functionalized to exhibit other functions such as targeted delivery and intrinsic fluorescence for bioimaging. NDs are unlike any other nanomaterial since not only can they provide all of the previously mentioned features, but these nanoparticles also exhibit excellent biocompatibility, mechanical stability, and unique optical properties. For instance, NDs can be utilized as both biomolecule carriers and as diagnostic tools, therefore unifying into a single platform the functionality of multiplexed nanoparticles. NDs possess a large specific surface area that enables a high drug loading capacity, coupled with a versatile surface chemistry that offers efficient binding of biomolecules to their surface. As with many other types of nanoparticles, NDs can not only increase the efficacy of cancer drugs by facilitating sustained release, but they can also bypass chemoresistance and preferentially accumulate in tumor cells due to the enhanced permeability and retention (EPR) effect attributed to the “leaky” vasculature of tumors [97]. The versatility and promising *in vivo* results of ND carriers for chemotherapy drugs, along with their superior biocompatibility over other nanomaterials such as carbon nanotubes, have recently encouraged researchers to study NDs for sustained and localized delivery of antibiotics, growth factors, and other biomolecules to augment tissue healing in regenerative medicine applications. With the rapidly expanding focus on gene delivery in regenerative medicine, researchers have most recently explored the use of NDs as multifunctional nonviral vectors for DNA, microRNA, and siRNA. Overall this section highlights the variety of therapeutics that NDs are capable of delivering, ranging from tumor-eradicating anthracyclines to gene-silencing siRNA, with a particular focus on the surface modification strategies necessary to develop such clinically relevant platforms.

3.1. Multifunctional carriers for cancer therapy

Delivery of Dox and similar tumor-eradicating anthracyclines has been a standard treatment for many forms of cancer, but systemic exposure of the body to these drugs results in deleterious side effects such as alopecia, myelosuppression, and cardiotoxicity. Chemoresistance of tumor cells further magnifies these side effects, since even though these drugs can readily be endocytosed by a tumor cell, they are quickly pumped back out of the cell by P-glycoprotein (Pgp), a transporter protein overexpressed in cancer cells. An estimated 90% of failed treatments for metastatic cancer are attributed to subpopulations of chemoresistant cells within tumors that avoid apoptosis by drug efflux [98]. The most effective solution to avoid chemoresistance is to conjugate the chemotherapeutic drug with nanoparticles to form nanocomplexes, which can evade drug efflux mechanisms since the drug in a complex is not recognized by Pgp. As the intracellular concentration of the conjugated drug increases due to a sustained release from the nanocarrier, the drug can successfully induce apoptosis and eradicate tumors [97]. The design of nanoparticle carriers for the improvement of cancer treatment is a fundamental goal in nanomedicine. Advantages of nanoparticle delivery for cancer drugs include an increase in drug efficacy and circulation half-life, a significant reduction in the required dosage, a decrease in side effects from systemic exposure, and the opportunity to link active cell targeting moieties and other biomolecules to the nanocomplex for targeted therapy [97].

Several nanoparticle-based delivery platforms for chemotherapeutic drugs have recently been FDA-approved or are undergoing clinical trials, ranging from liposomal carriers for Dox (Doxil®), to polymeric micelles for paclitaxel delivery (Genexol-PM®). Though effective by current clinical standards, these nanoparticle drugs still pose many risks or limitations that leave a large margin for improvement. Shi *et al.* provide a thorough review which evaluates the current status of cancer nanomedicine with comparisons of FDA-approved nanotherapies and their shortcomings that warrant the development of new nanoparticle carriers [99]. Carbon-based nanoparticles represent a promising class of inorganic nanomaterials with chemical and physical properties that can be tailored for highly efficient delivery of hydrophilic drugs. Carbon nanotubes (CNTs), which are one of the most widely researched carbon nanomaterials for cancer therapy, have been reported to enhance the efficacy of cancer drugs such as doxorubicin by suppressing the drug's toxic side effects and by bypassing chemoresistance. Despite these advantages, CNTs can induce undesirable cytotoxic side effects, and the lack of long-term studies on their toxicity in humans has prevented the study of this nanocarrier in the clinical setting [100]. However, a number of clinical studies have been conducted with more biocompatible carbon nanomaterials for cancer therapy, such as activated carbon nanoparticles, which were evaluated as nanocarriers for methotrexate in a 1996 clinical study for the treatment of gastric and esophageal cancers [101]. Additionally, carbon nanoparticles have been tested as a stain for healthy lymph node tissue in a 2015 clinical trial for enhanced surgical treatment of papillary thyroid carcinoma [102]. The success of both clinical trials indicates a promising role for biocompatible carbon-based materials in nanomedicine.

3.1.1. Self-assembling ND carriers for chemotherapy drugs—The use of NDs as a drug delivery platform was first demonstrated in 2007 with doxorubicin (Dox). In this study, NDs were presented as a facile yet robust platform capable of non-covalently loading Dox through the ionic interactions between the protonable amino group of Dox and the carboxyl groups of oxidized NDs, effectively entrapping the drug within ND aggregates. To facilitate the adsorption of this cationic drug to hydrophilic detonation NDs, the components were suspended in a sodium chloride solution, and the dissolution of Cl^- ions promoted the self-assembly of ND-Dox complexes. When administered to a colon cancer cell line *in vitro*, the release of Dox from ND-Dox was controlled by the local concentration of Cl^- ions in the cell media [89]. Upon further study of ND-Dox, the group reported that the NDs enhanced the cellular uptake and therapeutic efficacy of Dox when administered *in vitro* to several tumor cell lines. Subsequent *in vivo* studies in mouse models of mammary carcinoma and liver tumor revealed that ND-Dox was able to bypass the drug efflux resistance mechanisms of both types of cancer cells, increasing the circulation half-life of Dox by a factor of 10 [3]. Seven days after treatment, analysis of the extent of apoptosis of LT2-Myc liver tumors concluded that ND-Dox loaded with 100 μg of Dox induced nearly a 4-fold increase in tumor apoptosis compared with mice treated with the same dosage of unmodified Dox. In the more chemoresistant 4T1 mammary tumor model, a 10-fold increase in tumor apoptosis was observed in mice treated with ND-Dox compared to free Dox. ND-Dox also demonstrated enhanced retention of drug over time, with 1.5 μg of Dox per gram of tumor tissue present at 7 days, while in contrast free Dox was not detected after 72 hours. ND-Dox complexes were observed to be unaffected by the Pgp efflux mechanisms of chemoresistant

cells, and desorption of Dox from the nanocomplexes only occurred after cellular uptake, thus decreasing systemic exposure to the drug as well as eliminating deleterious side effects such as myelosuppression [3].

The use of NDs for their sustained release properties, improved retention in tumor tissue, reduction of systemic exposure to the drug, and ability to bypass chemoresistance has been studied for various other anthracyclines and chemotherapy agents such as epirubicin[2], paclitaxel[103], Purvalanol A, and 4-hydroxytamoxifen [104]. In these instances where the drug is loaded by physical adsorption, the release is often controlled by the pH of the surrounding media. Since the tumor microenvironment is well known to have a definitively lower pH than the rest of the human body, the design of controlled release systems, which retain cargo in normal tissues and release drug selectively in lower pH tumor tissues, is of great interest for cancer therapies. The major roadblock for the use of these self-assembling ND complexes in translational medicine is the strong affinity of NDs to aggregate. Several methods have been studied to improve the colloidal stability of ND carriers without compromising their multifunctional capabilities. By modifying the surface of NDs with polymers, lipids, or other biomaterials, the dispersivity and long-term colloidal stability of NDs is greatly enhanced. Furthermore, both non-covalent and covalent crosslinking strategies can be applied to also extend the functionality of NDs as drug or gene carriers.

3.1.2. Methods for improving the dispersivity of ND drug carriers—As discussed in the previous section on ND synthesis, nanoparticle aggregation is a significant challenge especially in the design and application of NDs for delivery of biomolecules. The strong tendency for NDs to form aggregates of 100–200 nm in diameter, and even micron-sized agglomerates, can prevent cellular uptake and endosomal escape of the loaded cargo [105]. One simple approach to address these challenges is to introduce a polymer or lipid coating to surfaces of nanoparticles to fabricate ND nanohybrids with controlled dispersivity and size [106]. Toward this goal, Xiao *et al.* incorporated a polyethylene glycol (PEG)-modified lipid onto ND-Dox complexes and reported that the lipid-modified complexes exhibited a higher circulation half-life and stability than uncoated ND-Dox when administered in mice [107]. By adsorbing a PEG-modified lipid to ND-Dox complexes, hybrid ND-lipid (NDL) particles were formed. The *in vivo* half-life of the drug from NDL-Dox in a murine lung-metastasized tumor model increased 8-fold from that of ND-Dox and 16-fold from that of unmodified Dox. In addition, the lipid-coated complexes facilitated a 3-fold and 12-fold increase in Dox accumulation in the lungs of mice as compared to unmodified Dox and ND-Dox, respectively. As a result of these functional improvements, NDL-Dox reportedly enhanced the treatment of breast cancer metastasis in the mouse model whereas ND-Dox caused a partial reduction in metastatic tumor volume.

PEGylation of ND-Dox has also been reported as an effective strategy to prevent aggregation of the nanocomplexes and can also provide further control over the release kinetics and circulation half-life of Dox both *in vitro* and *in vivo* [108–110]. Aside from polymer and lipid coatings, another strategy that has been implemented to improve the dispersivity of NDs for drug and gene delivery applications is covalent modification of nanodiamonds with amino acids. For example, carboxylated NDs were chemically conjugated with lysine through a carbon linker, and subsequent measurements with dynamic

light scattering (DLS) revealed the obtainment of particles with a size of 21 nm and narrow size distribution [9]. On the other hand, unmodified carboxylated NDs, which formed large aggregates up to the micron range, had a broad particle size distribution. The study also showed that the lysine-functionalized NDs could be further modified for loading and delivering bioactive molecules, such as siRNA.

3.1.3. Targeted NDs for cancer theranostics—Aside from improving the dispersivity and drug pharmacokinetics, lipid and polymer coatings on NDs can also serve as interfaces to which functional molecules such as cell-binding ligands can be grafted using common wet synthesis techniques including click chemistry and carbodiimide crosslinking. By chemically grafting antibodies, aptamers, peptides, or other ligands to the linking interface of an ND drug complex, the release of drug can be actively targeted with high specificity to tumorigenic markers.

When an ND complex is internalized by the targeted cell, the ligand first binds to the receptor on the cell membrane, and uptake occurs by receptor-mediated endocytosis. Several approaches to this concept include non-covalent lipid coatings, porous silica shells, and polymeric coatings. Finally, as an alternative strategy, ligands can also be grafted directly onto the surfaces of NDs.

Multifunctional biotin-modified lipid coatings are an attractive platform for non-covalently linking targeting molecules to NDs due to their self-assembly ability which eliminates the need for chemical conjugation. Such ND-lipid particles (NDLPs) were formed by rehydration of lipid films with NDs suspensions, and these nanohybrids exhibited improved dispersivity and presented a one-step linking strategy for the attachment of antibodies and fluorescent dyes [111]. Cell-targeted NDLPs were fabricated by the addition of biotinylated antibodies along with streptavidin to unmodified NDLPs. In this interaction, streptavidin serves as a cross-bridge in which one end binds to the biotin of the lipid film while the other end binds to the biotin in the modified antibody. As a proof of concept, NDLPs loaded with epirubicin (Epi) were targeted to a receptor that is overexpressed in breast cancer cells, epidermal growth factor receptor (EGFR). Biotinylated anti-EGFR was attached to NDLPs via streptavidin. Dye-loaded NDLPs were also fabricated to enable particle tracking by confocal microscopy to analyze nanocarrier localization. Cell studies *in vitro* revealed that the antibody-targeted NDLPs were rapidly internalized by EGFR-overexpressing breast cancer cells via EGF-mediated endocytosis, with nearly a 3-fold increase in cellular uptake compared to that of untargeted NDLPs. When the EGFR-targeted NDLP-Epi was administered *in vivo* for targeted delivery of Epi to a triple-negative breast cancer mouse model, a 50% greater reduction in tumor volume was observed 7 weeks after treatment, with respect to treatment with untargeted NDLP-Epi. In fact, the antibody-targeted NDLPs induced almost complete regression of tumors, while delivery of an equivalent dosage of free Epi resulted in mortality after 4 weeks of treatment [111]. Overall, the NDLP platform is a highly efficient and reproducible therapeutic and diagnostic platform. The aforementioned benefits in addition to their high biocompatibility and versatility toward loading nearly any type of drug and targeting molecule warrant further preclinical or clinical study. One downside that may limit its translational potential is that the self-assembly of the nanocomplex does not provide any control over critical synthesis parameters, such as

particle size. For instance, the addition of drugs, dyes, and streptavidin for antibody-linking can have a different impact on the diameter of the NDLPs, which is an issue that could hinder reproducibility and scalability.

Another reported technique to develop a multifunctional linker interface for NDs is the deposition of a porous silica coating onto NDs, which despite requiring a more complex synthesis procedure than the discussed NDLPs, enables precise control over the particle size and greater long-term colloidal stability. These silica coatings can vastly improve the drug loading efficiency due to the increase in surface area provided, and a polymer layer around the silica shell enables the chemical grafting of biomolecules including proteins, dyes, and targeting molecules by click chemistry [112, 113]. Furthermore, this approach is compatible with NDs produced by HPHT or by detonation. Optimization of the synthesis parameters also allows for deposition of silica shells at a precisely defined thickness that can be controlled within 10 nm. Slegerova *et al.* demonstrated the application of silica-coated FNDs for targeting of tumor cells (Figure 4A). Using click chemistry to immobilize cyclic RGD peptides to the copolymer-modified surface of the FND-silica composites, tumor-targeted complexes were prepared for delivery of a bioimaging probe to glioblastoma cells [114]. Glioblastoma is one of the several types of cancer cells that overexpress the integrin $\alpha_v\beta_3$, for which the synthetic cyclic RGD peptide has a high binding affinity. When delivered *in vitro*, the RGD-modified FND hybrids were rapidly endocytosed by U-87 MG glioblastoma cells, in contrast to untargeted FND hybrids. Confocal microscopy revealed that the RGD-modified FNDs were internalized by specific binding of FND complexes to $\alpha_v\beta_3$ followed by receptor-mediated endocytosis. This platform was also highly biocompatible, and the silica shell did not impact the fluorescent intensity of the NV^- centers in FNDs. Further studies on these FND-silica nanohybrids should evaluate the *in vivo* delivery and imaging capabilities for targeted cancer therapy. The versatility in the grafting techniques of both of the previously discussed preclinical studies presents a favorable modality for a combined delivery and bioimaging platform that can be targeted to multiple receptors to increase the uptake efficiency in cancer cells. For instance, Eph receptor tyrosine kinases are another class of receptors that are characteristic of tumor angiogenesis and are highly active during tumor development [115]. Eph receptor targeting peptides represent just one example of many other types of ligands which can be grafted to functionalized NDs or FNDs for targeting Eph-positive tumors as a diagnostic tool and drug delivery.

Bioactive molecules can also be immobilized directly to the surface functional groups of NDs, most commonly using carbodiimide crosslinking between carboxyl groups of NDs and amino groups of biomolecules. For instance, EDC-NHS coupling was used to link cisplatin, a chemotherapeutic drug, and the recombinant EGF protein to carboxylated NDs [116]. The resulting ND complexes exhibited specificity toward cells expressing EGFR, and by monitoring the Raman spectra of the NDs, the intracellular transport of NDs was tracked *in vitro*, confirming that the internalization occurred through EGFR-mediated endocytosis. While cisplatin delivery by untargeted NDs resulted in minimal inhibition of cell growth, EGF-modified NDs loaded with the same dosage of cisplatin significantly inhibited cell growth in HepG2 cells. Low doses (0.6 μg mL^{-1}) of cisplatin-loaded onto the targeted NDs inhibited cell growth to the same extent as high doses (5.0 μg mL^{-1}) of free cisplatin. A similar approach has also been evaluated for enhancing the efficacy of Dox by immobilizing

peptides on the surface of NDs (Figure 4B). Using NHS-EDC coupling, Dox and trans-activating transcriptional activator (TAT) peptide were both chemically linked to carboxylated NDs to form ND-Dox-TAT [117]. TAT is a cell-penetrating peptide that was originally derived from the HIV virus and has previously been shown to enhance cellular uptake of many types of nanoparticles. The conjugation of the TAT peptide to the surface of the ND effectively increased the rate of cellular translocation of the drug, and compared to ND-Dox, ND-Dox-TAT induced significantly higher cytotoxicity in glioma cells *in vitro*. Several other crosslinking strategies have shown promising results, for instance, sulfhydryl-reactive crosslinking chemistry was used to link thiolated paclitaxel and thiolated monoclonal anti-EGFR with fluorescent oligonucleotide labels to NDs to develop a tumor-targeted ND carrier for paclitaxel with simultaneous bioimaging capabilities [118].

A recent study showed that NDs are not only capable of targeting a single receptor, but their high surface area and chemistry enable the loading of multiple ligands at once to achieve dual-targeted delivery and particle tracking. Chan *et al*. demonstrated this concept with ND-Dox to facilitate both active cell targeting of chemoresistant breast cancer cells as well as subcellular targeting after internalization to sequester Dox to the mitochondria and bypass Pgp-mediated efflux [119]. Dually-targeted ND-Dox complexes were formed by chemical conjugation of NDs with folic acid (FA) in addition to mitochondrial localizing sequence (MLS) peptides. FA is a commonly utilized ligand for the folate receptor, which is overexpressed in most cancer cells. MLS peptides were recently identified to enhance the efficacy of Dox by targeting the subcellular delivery of the drug to the mitochondria of the cell and entirely bypassing drug efflux. This platform was assembled by linking PEGylated FA and MLS peptides to carboxylated NDs through EDC/NHS coupling to create dually-targeted NDs, (FA-MLS)-NDs, with a 6 to 1 ratio of FA to MLS. Afterward, Dox was loaded to the (FA-MLS)-NDs by physical adsorption with a 75% loading efficiency, forming (FA-MLS)-ND-Dox complexes. The *in vitro* study concluded that upon administration of (FA-MLS)-ND-Dox to MCF-7 human breast cancer cells, the complexes were selectively internalized by folate receptor and then localized directly into cells' mitochondria. In contrast, the delivery of Dox by (FA)-ND-Dox resulted in receptor-mediated uptake followed by nonspecific localization of drug in the lysosomes of the cells. In MCF-7/ADR cells, a human cancer cell line which overexpresses P-gp, administration of (FA-MLS)-ND-Dox containing 10 μM Dox resulted in approximately 70% cell death within 2 days, whereas administration of 10 μM of unmodified Dox or with (FA)-ND-Dox induced approximately 5% cell death. Interestingly, when Dox was delivered with FA-tagged NDs, the rapid efflux of the drug counteracted the potential benefits of ND delivery, thus highlighting the potential therapeutic benefit of subcellular targeting *in vivo*.

3.2. Gene delivery

Gene therapy is the increasingly popular strategy of inducing or silencing the expression of targeted genes to treat or diagnose diseases. Genes are transferred to cells in carriers known as vectors, and successful gene therapy requires the design of efficient and biocompatible vectors that mediate the cellular uptake of genetic material. While viral gene delivery is highly effective, several safety concerns have limited their clinical application. The success of NDs as a drug delivery platform has encouraged researchers to investigate the efficacy of

NDs as a nonviral vector for gene delivery. To design an ND vector to deliver plasmid DNA or small interfering RNA (siRNA), NDs must be functionalized to create a cationic surface to which negatively charged DNA or siRNA can adsorb and desorb. For example, polymers such as polyethyleneimine (PEI) or poly(allylamine hydrochloride) (PAH) were adsorbed to the surfaces of carboxylated NDs to form ND-polycation complexes ND-PEI and ND-PAH [120]. PEI is a cationic polymer that is commonly studied for its high affinity to bind to DNA and siRNA, but when delivered alone its transfection efficiency is low because it is not readily internalized by cells. By complexing these polymers with NDs, which are internalized by cells via endocytosis, highly efficient vectors can be developed. Both ND-PEI and ND-PAH demonstrated high loading efficiencies for the adsorption of siRNA, and when delivered to Ewing sarcoma cells, ND-PEI exhibited a higher transfection efficiency than ND-PAH for the knockdown of an oncogenic marker. Additionally, both PEI and PAH-modified NDs displayed a higher transfection efficiency and much lower cytotoxicity than Lipofectamine, a very popular lipid-based non-viral vector. Alhaddad *et al*. also demonstrated that the same complexes could be formed with fluorescent NDs (FNDs), enabling the possibility to track the delivery of the vectors in real time using confocal microscopy [120]. Polycation complexes formed with FNDs enabled fluorescent imaging of siRNA transfection, revealing that cells internalized the ND vectors by endocytosis. Chen *et al*. have similarly investigated the use of ND-PEI complexes for siRNA delivery [121]. By adsorbing 800 Da PEI to carboxylated NDs, ND-PEI vectors were formed which possessed a high loading capacity and promoted a sustained release of siRNA. When delivered *in vitro* to GFP-expressing M4A4 cells, ND-PEI vectors induced a 62.2% knockdown of GFP expression at 48 hours with negligible cytotoxicity to the cells, in contrast to Lipofectamine which caused a 26.4% reduction in cell viability to achieve similar knockdown levels.

Though non-covalently linked, self-assembling ND-polycation complexes have shown promising results as efficient and biocompatible vectors, the long-term stability of these complexes in suspension and the aggregation of NDs are two main challenges that limit their therapeutic potential. Thus, ND vectors formed by chemical conjugation may be preferable for the development of stable and well-dispersed DNA and siRNA carriers. One strategy is the covalent modification of NDs with lysine to introduce a cationic surface charge to readily adsorb siRNA and prevent particle aggregation. siRNA was loaded onto lysine-modified NDs by physical adsorption, and when delivered *in vitro* to HeLa cells the complexes facilitated a high transfection efficiency with negligible cytotoxicity [122]. Interestingly, the lysine-functionalized NDs were observed to bind to physiological proteins which formed a layer of adsorbed proteins on the siRNA vectors that enhanced the dispersivity of the vectors and had a positive impact on cellular uptake. Alternatively, Zhao *et al*. investigated the covalent attachment of polypeptides to polyglycerol (PG)-modified NDs to create highly-dispersed and positively charged conjugates [123]. Through click chemistry, positively-charged polypeptides were chemically conjugated with PG-NDs to form DNA vectors that were well-dispersed in solution.

Another benefit of chemical conjugation in developing ND-based vectors is the ability to achieve targeted gene delivery by linking NDs with cell-targeting ligands as described previously for targeted drug delivery. One technique for creating tumor-targeted NDs for siRNA delivery was achieved by covalently linking RGD peptide to functionalized NDs

which were used as vectors for delivering VEGF siRNA to silence the expression of VEGF protein in cells [124]. Briefly, NDs were carboxylated and then reacted with thionyl chloride to create highly reactive surface moiety to which the RGD peptide was covalently linked once the protecting groups of the peptide were removed in dimethylformamide. The resulting RGD-ND vectors were loaded with VEGF siRNA, and over 250 hours after delivery to HeLa cells *in vitro*, an estimated 50% of the loaded siRNA was released. The sustained release of siRNA is beneficial for the therapeutic use of gene silencing, because siRNA is quickly degraded by enzymes in the cytoplasm [124]. In comparison to Lipofectamine, which silenced VEGF expression by 34%, RGD-ND vectors had a significantly higher efficacy with 63% inhibition of VEGF expression. RGD-ND vectors were also observed to inhibit tumor growth *in vivo* by VEGF gene silencing in a mouse xenograft model. The vectors were delivered *in vivo* by IV injection to mice, and the covalent attachment of RGD peptide resulted in a 150% higher concentration of vector in tumor cells as opposed to all other organs. The strategy used for surface linking the peptide was vital for the successful targeting of the vector. In fact, the group showed that covalent ND-peptide conjugates maintained stability even after 240 hours of storage in suspension, and only 10% of the peptide was released. In contrast, non-covalent linkage of the peptide, by physical adsorption of RGD to the NDs, formed complexes which released all of the loaded peptide within 50 hours [124]. Bi *et al.* further demonstrated the utility of the peptide-targeted NDs for delivering siRNA to silence the survivin gene, which is an apoptosis inhibitor that can be used as a therapeutic target for cancer treatment [125]. The RGD-linked NDs carrying survivin siRNA inhibited tumor growth *in vivo* in a mouse model to the same extent as a therapeutic dose of Dox.

3.3. Localized delivery for regenerative medicine applications

Although NDs have primarily been evaluated as a therapeutic and diagnostic tool for cancer, NDs also have great potential for wound healing and regenerative medicine therapies that require controlled delivery of biomolecules that is localized to the site of wounds or damaged tissue.

In addition to cancer drugs, antibiotics can also be delivered using NDs to improve their therapeutic activity and lower the required dose needed for a successful treatment. Particularly in the case of antibiotic-resistant infections, such as methicillin-resistant Staphylococcus aureus (MRSA), high doses of antibiotics are required to treat the infection, due to the reduced effectiveness of the drugs in killing the rapidly growing number of antibiotic-resistant strains of bacteria. In addition, some antibiotics such as vancomycin can reportedly induce nephrotoxic and ototoxic effects in high doses, which could be prevented with a targeted or sustained delivery system [126]. NDs offer a potential solution for increasing the efficacy and therefore reducing the required loading dose of antibiotics. Moreover, the drug shielding properties of ND complexes can greatly minimize systemic exposure and undesired side effects. Recent studies have highlighted the success of NDs for delivery of antibiotics such as vancomycin, tetracycline, and amoxicillin [127, 128]. The drug complexes, which were formed non-covalently using carboxylated or aminated NDs, demonstrated sustained drug release in a pH-dependent manner. As the pH of the

surrounding microenvironment changes, an alteration in the charge distribution on the surface of NDs results in the adsorption or desorption of the drug.

Growth factors and proteins represent another important class of therapeutics that can be delivered by NDs with a sustained release not only for treating disease but also for improving the therapeutic efficacy of tissue scaffolds. Growth factors can be used to treat and target many diseases, but their short half-lives and rapid clearance have hindered their success. Clinical use of growth factors, such as the delivery of bone morphogenetic protein 2 (BMP-2) for bone regeneration, can frequently induce adverse side effects such as heterotropic bone formation, edema, and even cancer, since effective treatment without sustained delivery requires dangerously high dosages to be administered [129]. With a high affinity for adsorbing proteins, NDs provide a straightforward and cost-effective solution for improving current growth factor treatments. The tunable surface chemistry of NDs also facilitates the covalent linkage of growth factors to the surface of the nanoparticle.

The most commonly employed strategy for loading proteins onto NDs is physisorption of the protein to the surface of the NDs [130]. For instance, insulin was observed to readily bind to the surface of NDs that contained hydroxyl and carboxyl surface groups, and the release of insulin was proportional to the pH of the aqueous environment [131]. At very high pH values the electrostatic forces between the insulin and the hydroxyl and carboxyl surface groups of the NDs were disrupted by electrostatic repulsion, causing the desorption and release of insulin from ND complexes. Moore *et al.* investigated a similar pH-dependent release of the growth factors BMP-2 and basic fibroblast growth factor (bFGF) with ultra-dispersed NDs [132]. The study found that both growth factors could be reversibly loaded and released from NDs by physisorption and desorption, respectively, in a pH-dependent manner. The *in vitro* cell studies confirmed the dual release of BMP-2 and bFGF, which resulted in osteogenic differentiation when delivered to myoblasts. The pH-dependent release kinetics allow the potential use of this technology in oral surgery to provide sustained bone regenerative therapy since the slightly acidic pH of the mouth could trigger desorption. Other growth factors, such as vascular endothelial growth factor (VEGF), can also be successfully linked to NDs by physisorption to provide a sustained and pH-dependent release of the protein [133]. Physisorption is often preferred over covalent linkage for loading growth factors to NDs since it can be completed in a simple procedure without chemical modification. Furthermore, covalent linkage to NDs can potentially degrade or inactive growth factors. In a comparative study of BMP -2 released from either non-covalent or covalently formed ND complexes, the non-covalent complex displayed sustained BMP-2 release for over 70 days while covalent conjugation resulted in minimal release and also inactivation of the BMP-2 [129].

Finally, a growing body of research focuses on combining NDs with biomaterial scaffolds or substrates to facilitate a localized release of growth factors and promote a superior healing response when the construct is implanted into a wound site. The success of such strategies depends both on the design of NDs as a carrier, as described here, and furthermore on the design of the scaffold into which the ND complexes are incorporated. The role of biomolecule-eluting ND scaffolds in the field of regenerative medicine will be discussed in further detail in Section 4.4.

4. Tissue engineering

Tissue engineering is a multifaceted field based upon the development of tissue scaffolds, which are biomaterial templates or substrates that control cell migration, adhesion, and differentiation to restore damaged tissues or organs [134]. In addition to supporting cellular activities, successful scaffolds must provide mechanical support for tissue growth and maintain biomechanical stability similar to that of native tissue. Above all, the design of an efficient tissue scaffold requires careful selection of biocompatible polymers and nanomaterials that do not interfere with biological processes such as cell division or differentiation. The biocompatibility, stability, hardness, wettability and optical properties of NDs in addition to their versatile surfaces which can be loaded with virtually any type of biomolecule are all favorable properties that enable their use as multifunctional materials in biomedical constructs. NDs are unique from other biomaterials in their ability to provide all of these traits as a single nanomaterial, which has inspired researchers to investigate NDs for a broad range of applications in regenerative medicine with a particular focus on bone and neural tissue engineering. Recently, NDs have been utilized as cell-adhesive surface coatings for scaffolds, as coatings to improve tribological properties of implants, and as nanofillers to reinforce the mechanical properties of composite scaffolds. Finally, several emerging trends in ND-based tissue engineering will be discussed, in regards to the strategies that incorporate NDs as a multifunctional delivery platform in scaffold matrices.

4.1. Cell substrates

The unique physical and chemical properties of NDs have prompted tissue engineers to utilize NDs and ND composites as cell substrates that can be designed to control cell adhesion and proliferation. For instance, the unique nanoscale properties of NDs, specifically their surface charge distribution facilitates the physical adsorption of cell-adhesive serum proteins to the surface of the nanoparticle, and this resulting cellular interface has been investigated for use primarily in bone regeneration and more recently for neural tissue engineering. The adsorption of serum proteins such as fibronectin (FN) and vitronectin (VN) to NDs allows the adhesion of a variety of cell types, and furthermore the surface chemistry and topography of NDs can be exploited to control cell functions such as differentiation [135–137]. These cell-adhesive properties can be introduced to biomedical implants through a variety of scalable and reproducible methods of depositing layered coatings and films of NDs. One popular technique is CVD, which uses plasma to deposit thin films of NDs with a tunable topography onto substrates and scaffolds [137]. CVD has been used to form surface coatings with DNDs and many other types of functionalized NDs, such as electrically-conductive boron-doped NDs [137].

To study the effects of surface chemistry on cell interactions, DNDs of differing hydrophilicity were deposited onto substrates by CVD, onto which rat mesenchymal stem cells (rMSCs) were seeded. Interestingly, the more hydrophilic DND films promoted osteoblast adhesion and increased ALP expression in rMSCs [138]. One likely explanation for this phenomenon is that the conformation of bound serum proteins like FN depends on the hydrophilicity of the substrate, and the cell-binding domains of FN are hidden when the protein is bound to a hydrophobic surface [139]. Thus, developing ND coatings with

hydrophilic surfaces by using oxygen-terminated NDs, is an effective design to maximize the biological activity of an implant. To demonstrate this concept *in vivo*, Xing *et al.* developed a poly(LLA-*co*-CL) (PLCL) bone scaffolds coated in carboxylated NDs, and 24 weeks after implantation into defects in sheep calvaria, the ND-coated scaffolds reportedly facilitated complete regeneration of the defects [34]. In contrast, unmodified PLCL scaffolds showed minimal bone restoration after 24 weeks. The *in vitro* results of the study concluded that the use of NDs as a surface coating on PLCL scaffolds resulted in the upregulation of osteogenic markers in human BMSCs [34].

Similarly, in another study the inclusion of acid purified detonated NDs in the same type of synthetic scaffold made of poly(LLA-*co*CL) was beneficial in promoting osteogenic differentiation by modulating the superficial properties of the scaffold [140]. Specifically, the presence of NDs altered the surface topography, which had a profound effect on protein adsorption. For instance, the alteration in the nanoscale roughness induced by NDs caused an increase in the seeding efficiency of BMSCs and a decrease of albumin adsorption, which is beneficial in reducing the activation of macrophages that can form a fibrous capsule on the scaffold surface. Moreover, the presence of oxygen functional groups on the NDs, such as carbonyl and lactone groups, increased the hydrophilicity of the surface of the poly(LLA-*co*CL) scaffold. This change in this parameter as explained above can promote selective adsorption of proteins in their native conformation enabling higher BMSCs adhesion and stem cell proliferation.

Due to their favourable surface properties so far described, NDs have been also investigated in combination with other bioactive materials to enhance the process of cell adhesion. For instance, hydroxyapatite inherently possesses osteoinductive properties, and when deposited into a film coating with oxidized detonation NDs, its ability to promote osseointegration *in vitro* was enhanced even further [135]. The presence of various positively charged functional groups on the surface of the NDs was found to greatly enhance the overall adsorption of FN to the AP-ND coatings in contrast to AP and stainless steel coatings. AP-ND coatings also showed preferential adsorption of FN over other proteins when incubated with serum-containing media. While the addition of NDs to AP coatings did not affect the nanoscale architecture of the coating, the addition of NDs altered the surface charge and therefore the hydrophobicity of the substrate. When tested *in vitro* with human osteoblast-like MG-63 cells, the serum-incubated AP-ND coatings promoted a significantly greater extent of osteoblast adhesion compared to AP and stainless steel substrates alone. In the absence of serum, cells did not show a preference for adhering to either type of substrate. Thus, as concluded in the study, the addition of NDs to electrodeposited AP coatings indirectly enabled osteoblast adhesion due to the increased presence of adsorbed FN because of the presence of NDs. In addition to promoting formation of focal adhesions between osteoblasts and the AP-ND substrate compared to AP substrate, osteoblasts also demonstrated an enhanced ability to reorganize FN when studied on the substrates with NDs (Figure 5A).

Aside from enhancing the bioactivity of bone scaffolds, NDs have also recently been identified as a highly used tool for neural tissue engineering. Similarly to osteoblasts, neurons and nerve cells have also been discovered to adhere and proliferate on NDs films and monolayers [141]. Traditionally, the *in vitro* culture of neurons requires substrates that

are laminated with ECM proteins such as ornithine and laminin or with synthetic substrates such as polylysine (PLL). PLL and other similar synthetic biomaterials are cytotoxic and therefore cannot be used for *in vivo* applications. NDs have been identified as a potential neural cell substrate that can be used to develop implantable and biocompatible neural prosthetics. Although a significantly larger body of research already exists on the applications of CNTs as substrates for neurons, the potential toxicity of CNTs is a crucial factor that will limit their use in future clinical implants. CNTs have also been reported to alter intraneuronal transport mechanisms and affect information processing throughout neural networks [142]. In contrast, NDs are reported to have no effects on the backpropagation of action potentials.

Preliminary studies found that monolayers of oxygen-terminated DNDs supported the adhesion and neurite extension of primary hippocampal neurons to the same extent as synthetic laminin-(poly-DL-ornithine) control substrates [141]. Neurite branching, which is required for the formation of functional neuronal circuits, occurred on the ND substrates with no differences from the control substrate, and synaptic transmissions were observed among both the ND and control substrates. Edgington *et al.* correlated neural cell adhesion and neurite extension with the morphology of the NDs; substrates composed of smaller and rounder NDs, mimetic of ECM proteins, generated denser neural networks [143]. Furthermore, the surface chemistry of the NDs did not have a noticeable effect on neurite extension in neuron cultures on monolayers of either oxygenated or hydrogenated NDs. Rather than a direct interaction between the cells and the nanoparticles, the mechanism of adhesion is likely due to the highly physisorption nature of NDs resulting in the adsorption of serum proteins such as FN or VN, to which neurons can bind. Toward the creation of patterned neural networks, the group further demonstrated that photolithography masks and reactive ion etching could be used to deposit high contrast (<10 μm) patterns of NDs onto substrates to form microscale patterns of NDs. Neurons adhered to the micropatterned substrates and successfully formed neurite branches that extended only throughout the patterned regions [143]. (Figure 5B)

Further studies have been conducted which show that a variety of neural cell lines can be cultured on ND substrates. For instance, amino-functionalized NDs have also been shown to support neural cell adhesion for neuroblastoma-glioma, Schwann, and dorsal root ganglion (DRG) cells [144]. All three cell lines formed dense neural networks and neurite extensions on the aminated ND substrates over long periods of culture (3 weeks). Electrically conductive ND substrates can also be obtained by boron-doping of ND [145]. Full factorial studies should be conducted in the future to gain further insight on the role of substrate topography and surface chemistry on the adhesion of both bone and neural cell lines.

4.2. Implant surface coatings

In addition to their use as cell-adhesive substrates, the advantageous tribological properties of NDs can be used to improve the wear resistance of joint prosthetics. Long term wear of hip, knee, and other joint replacement implants results in the formation of small debris particles that accumulate and cause joint pain, osteolysis, implant loosening, and ultimately implant failure [147]. ND coatings have been demonstrated to improve the wear resistance

and prevent metal ion leaching from cobalt-chromium-molybdenum (CoCrMo) hip and knee implants, titanium temporomandibular joint implants, and titanium dental implant screws [148–152]. Diamond-like coatings have also been shown to improve the biocompatibility of metal coronary artery stents by preventing the release of metallic ions [153]. As simulated *in vitro*, the average volume of wear debris per year from metal-on-metal CoCrMo implants was 5 mm^3. The hip implants with ND coatings produced 50,000 times less wear debris per year compared to the uncoated implants [154]. ND implant coatings have also shown promising *in vivo* results. In one model, ND coatings applied to Ti-6Al-4V implants greatly enhanced their osseointegration within femoral defects in rabbits [155].

4.3. Nanofillers in polymer composites

Successful tissue scaffolds require materials that degrade at a controlled rate to allow the ingrowth of new tissue. Additionally, a scaffold must possess mechanical properties that are either equivalent or superior to that of the tissue being restored. Polymers are a favored biomaterial used to construct tissue scaffolds because they can form biomimetic structures that resemble the hierarchal architecture of native tissue with precisely tunable degradability. However, polymers are limited by their weak mechanical properties. With a high surface area to volume ratio and the abundance of reactive functional groups on their surfaces, NDs have the ability to serve as nanofillers to reinforce the mechanical properties of polymers and create multifunctional nanocomposites that can be designed for use in soft tissue as well as hard tissue regeneration [106]. Among the various techniques to produce scaffolds, electrospinning is a popular strategy for creating polymeric nanofibers that mimic the native ECM architecture. Salaam *et al.* demonstrated that the mechanical properties of electrospun poly(ε-caprolactone) (PCL) scaffolds were reinforced with DNDs at various loading concentrations [156]. PCL containing 0.1 wt% DNDs exhibited a tensile modulus of 108.5 MPa which is comparable to that of human cancellous bone. Plain PCL, in comparison, displayed a significantly lower tensile modulus of 85.4 MPa. At greater DND concentrations, no improvements in mechanical properties were observed which may be due to a percolation threshold effect, or simply due to nanoparticle aggregation at higher concentrations. Polyvinyl alcohol (PVA) is another polymer which has been investigated as a bone scaffold material by reinforcement with carboxylated NDs [157]. The addition of 2 wt % NDs to PVA nanofibers resulted in a reported 89% increase in tensile strength and 155% increase in Young's modulus from unmodified PVA nanofibers. At nanofiller concentrations above 2 wt%, the addition of NDs did not enhance the mechanical properties of the polymeric scaffolds due to the affinity of NDs to aggregate at higher concentrations. Brady *et al.* showed that electrospun PLGA nanocomposite bone scaffolds could be reinforced by the addition of DNDs [158]. PLGA nanocomposites with 2.3 wt% DNDs exhibited a two-fold increase in both elastic modulus and hardness. Aside from their use as nanofillers for bone tissue engineering, NDs have also been investigated for their nanofiller properties in polymeric scaffolds for wound healing. Toward the development of biopolymer films with properties similar to skin, medical grade NDs were added to chitosan and bacterial cellulose polymers to increase the tensile strength of electrospun membranes [159]. The addition of 1 wt% of NDs increased the uniaxial tensile strength from 13 MPa to 25 MPa, and the resulting increase in hydrophilicity by the NDs improved cellular adhesion to the scaffolds.

Above a concentration of 1 wt%, aggregation of NDs suppressed any further enhancements in mechanical properties.

Each of the previously described studies of NDs as nanofillers reported a common finding: NDs can reinforce polymeric matrices and electrospun nanofibers over a wide range of mechanical properties to create soft tissue mimetics for wound dressing or hard tissue mimetics for bone scaffolding; however nanoparticle aggregation remains a significant challenge. In high concentrations, the mechanical properties of the polymer are no longer enhanced because the functional groups of the NDs begin to interact with each other rather than with the polymeric network. To circumvent this and further reinforce polymer properties, NDs can be covalently modified to increase their long-term stability and dispersivity. One approach has been demonstrated by the incorporation of amino-functionalized NDs into epoxy resins which resulted in the covalent conjugation of the epoxy and the reactive $–NH_2$ on the NDs [160]. Amino-functionalized NDs were prepared from detonation soot by carboxylation followed by reaction with thionyl chloride to enable the linking of ethylenediamine. The resulting polymeric nanocomposites formed by covalent linkage displayed a 50% increase in Young's modulus and a 300% increase in hardness compared to nanocomposites formed with carboxylated NDs, which did not form covalent bonds with the epoxy [160]. Similar benefits were observed with PLLA nanocomposites formed with NDs that were covalently linked to a surfactant to enhance stability and dispersion [82]. NDs were chemically conjugated with octadecylamine (ODA) to form ND-ODA complexes that reportedly improved mechanical properties of PLLA at concentrations up to 10 wt% of ND-ODA. With respect to pure PLLA scaffolds, PLLA containing 10 wt% ND-ODA showed a two-fold increase in Young's modulus and an 8-fold increase in hardness. In fact, these nanocomposite scaffolds showed equivalent mechanical properties to human cortical bone. Zhang *et al.* also demonstrated that phospholipid-coated NDs could be incorporated into PLGA scaffolds to achieve a 100% increase in Young's modulus and 550% increase in hardness compared to scaffolds made of pure PLGA [161]. At 20 wt% NDs, the nanocomposites possessed mechanical properties that matched that of cortical bone. The ND-based nanocomposites supported cell growth and did not invoke an immune response when implanted *in vivo* in mice.

4.4. Biomolecule-eluting scaffolds

An emerging strategy in tissue engineering with NDs is to utilize their full potential both as a nanofiller as well as a delivery platform to create multifunctional bioactive scaffolds that release therapeutic biomolecules to improve the *in vivo* healing response. The previously described functions of NDs as a growth factor release platform can be introduced to tissue scaffolds to achieve therapeutic benefits to accelerate the healing response. Copolymers commonly used in bone tissue engineering, such as PLCL, have been coated with NDs loaded with BMP2 to improve the osteogenic function of the implant [129]. The incorporation of ND complexes facilitated sustained release of BMP -2 from the scaffold *in vivo*, which was measured by the upregulation of osteogenic markers *RUNX2*, *COL1A2*, and *COL2A1*. Furthermore, the ND coatings displayed localized anti-inflammatory effects due to their function in inhibiting the adhesion of inflammatory cells [129]. A subsequent study from the same group studied the osteogenic functions and tumorigenic potential of the

PLCL scaffolds coated with NDs and the same scaffolds coated with ND-BMP complexes [162]. The presence of the hydroxylated NDs on the surface of the scaffolds was reported to cause a significant reduction in tumor growth when administered *in vitro* to dysplastic oral keratinocytes. The presence of NDs similarly caused a decrease in tumor size 8 weeks after the scaffolds were implanted *in vivo* in a mouse oral carcinogenesis model, possibly due to the ND-induced differentiation of tumor cells. On the other hand, the scaffolds coated in ND-BMP complexes, which facilitated a sustained release of BMP-2, caused an increase in invasive tumor growth due to the activity of the BMP-2. Since a direct link between BMP-2 signaling and cancer has not been identified, the cause of the observed increase in tumorigenic potential in ND-BMP coated scaffolds is unknown and warrants further investigation. These results also suggest the possible benefits of ND coatings both in terms of promoting osteogenic function as well as inhibiting tumor growth. ND surface coatings have also been used for the sustained release of angiogenic growth factors from β-tricalcium phosphate (β-TCP) scaffolds to improve their bone healing capacity [163]. After linking VEGF and Ang-1 non-covalently to oxygenated NDs, the ND complexes were deposited onto β-TCP scaffolds which were implanted into osseous defects in sheep calvaria. Compared to control scaffolds which were not coated with NDs, scaffolds coated with ND-Ang displayed significantly increased blood vessel densities both at 1 and 3 months after implantation. The effects of the ND-Ang surface coatings were also observed by an increase in blood vessel diameter.

5. Bioimaging

Biological labeling is a powerful technique for visualizing the dynamics of biological systems, and this multidisciplinary field not only enables researchers to track cell behavior with nanoscale precision *in vitro* and *in vivo*, but it also allows clinicians to noninvasively diagnose cancer and other diseases. Thus, researchers and clinicians alike require biocompatible and cost-effective probes that remain photostable and easily distinguishable from cells or tissues over long time scales. Though an extensive selection of fluorescent probes is available in both lab and clinic, there is still a high demand for more effective and multifunctional fluorescent markers. A new modality of modern medicine is the use of combined therapeutic and diagnostic (‘theranostic’) platforms to create advanced nanocarriers which enable simultaneous tracking and treatment strategies. This concept of multimodal imaging and treatment unifies the goals of both researchers and clinicians, yet a probe that is compatible for widespread use in both the laboratory and the clinic is not readily available.

A promising tool that can bridge this existing gap is represented by fluorescent NDs (FND), which possess a set of unique properties that cannot be found in conventionally available probes. Since their discovery, FNDs have been investigated for a variety of applications including drug and gene delivery, tracking the long-term fate of stem cells *in vivo*, developing disease models, and for designing diagnostic probes for detecting and monitoring diseases. To define their value as theranostic platforms and their potential use in clinical settings, this section will discuss the ongoing efforts in the use of FNDs in three main emerging areas including subcellular imaging, cell labeling and magnetic resonance imaging (MRI).

5.1. Subcellular imaging with FNDs

Fluorescent nanodiamonds (FNDs) have recently emerged as a promising theranostic probe that offers advantages including biocompatibility, long-term stability, and strong fluorescent signal. FNDs emit a fluorescent signal due to the presence of nitrogen-vacancy (NV) centers which are defects in the sp^3 carbon lattice of NDs. Several distinctly structured centers can be formed depending on the structure of nitrogen impurities within the diamond. However, the scope of this discussion will be limited to negatively charge (NV^-) vacancy centers which absorb light at 550 nm and emit an intense far-red signal at 685–700 nm [90, 91, 164]. NV^- centers, which consist of a nitrogen atom paired with a lattice vacancy in place of a carbon atom, are formed by irradiating NDs with electrons or ions followed by thermal annealing to immobilize the NV^- centers [90].

FNDs possess several unique properties with respect to other standard fluorescent probes. Firstly, the fluorescence lifetime of FNDs containing NV^- centers is on average 5 to 7 fold greater than that of biological tissue [165]. This significant difference offers a great advantage because it facilitates background-free imaging of particles within cells and tissues. Additionally, FNDs do not photobleach and are more photostable when compared to other commonly used probes, such as QDs [166, 167].

These properties enable analysis at a high spatial resolution that is essential for single particle tracking (SPT) of biomolecules on a subcellular scale. SPT is a useful strategy in biomedical research not only for identifying cellular processes but also for studying abnormalities in cellular functions caused by a disease. A recent investigation showed the use of FNDs in SPT as a probe for detecting abnormalities in neuronal transport. Notably, this report by Haziza *et al.* is the very first nanoparticle-based platform used to enable direct measurement of intraneuronal transport *in vivo* [168]. The group was able to track the motion of FNDs inside neurons, both *in vitro* and *in vivo* to develop a high-throughput assay measuring intraneuronal transport. By delivering FNDs to primary hippocampal neurons, the subcellular transit of FNDs was captured in real time using pseudo-total internal reflection fluorescence video microscopy (pseudo-TIRF). From the pseudo-TIRF analysis, the motion of the FNDs was correlated to parameters which characterized anterograde and retrograde intraneuronal transport. These correlations served as the foundation for a novel high-throughput assay for screening genetic markers and drugs that impact neuronal transport. The high biocompatibility, stability, and fluorescence lifetime enabled long-term background-free fluorescent imaging and precise localization (>12 nm) of FND trajectories throughout neuronal microtubules. The FND tracking assay was used to study the changes in neuronal transport caused by Alzheimer's disease, which is known to impair neural activity by the accumulation of amyloid plaques. The FND tracking assay was applied to *in vitro* cultures of primary hippocampal neurons that were treated with amyloid-$\beta_{1–42}$ peptide, and effectively demonstrated amyloid-mediated impairment of intraneuronal transport by various parameters such as the decreased transport velocity of FNDs. (Figure 6A). The study also tested the FND-based assay for screening the pharmacological effects of drugs. For instance, FND tracking revealed a dose-dependent trend in the nanomolar range with the model drug nocodazole on its impairment of intraneuronal transport. The FND tracking assay was also demonstrated *in vivo* in transgenic mice to assess the impact of genetic factors associated

with Alzheimer's and autism on intraneuronal transport. In mice with the transgene *Mark1*, which is related to Alzheimer's, FND tracking was able to detect even small changes in microtubule-associated protein (MAP) concentrations due to *Mark1* expression. FND tracking also revealed an impairment of intraneuronal transport caused by the expression of *SCL25A12*, a genetic marker associated with autism.

In addition to monitoring transport within cells, the high-resolution particle tracking enabled by NV^- centers in FNDs can be used to evaluate transmembrane signaling. By identifying ligand-receptor binding and activation of signaling pathways, FNDs can be utilized as a platform to screen receptor-targeting drugs. One strategy showed the efficacy of FNDs as a protein tag for 3D molecular imaging to test the effects of small molecule kinase inhibitors (SMIs) on transmembrane signaling of endogenous proteins [169]. Streptavidin-bound PEG was covalently linked to carboxylated FNDs by EDC-NHS coupling. Biotin-modified TGF-β was then linked to the PEGylated FNDs through streptavidin, forming the FND-TGF complex, which was further functionalized with bovine serum albumin (BSA) to prevent aggregation. 3D localization microscopy enabled the tracking of FND-tagged TGF-β within cells, which was accurate within 8 and 16 nm on the x and z-axes, respectively. The fluorescent tag allowed for real-time imaging of the protein binding with the TGF receptor on the cell, prior to its internalization into the cytoplasm. 3D localization further enabled the analysis of the protein's diffusion trajectory through the cell membrane, and the change in diffusion kinetics upon treatment of cells with an SMI targeted to TGF-β kinase. (Figure 6B). FNDs have also proven to be useful tools for labeling surface receptors on cells. For instance, polyglycerol-modified FNDs were used to fluorescently label interleukin-18 receptor α (ILRα) on the surfaces of HEK293 cells to reveal the subcellular diffusion trajectory upon receptor binding [170]. Targeted FNDs have also been used to track the interactions between transferrins and their corresponding receptors on HeLa cells [171].

Although SPT is most frequently applied to study the signaling or transport of molecules through individual cells, it has also been used to study transport between cells. Specifically, FNDs have been used to track the transport of proteins between human embryonic kidney (HEK293T) cells and neuroblastoma (SH-SY5Y) cells through a recently identified transport mechanism between cells known as tunneling nanotubule transport (TNT) [172]. By adsorbing model proteins such as BSA and green fluorescent protein to carboxylated FNDs, TNT-mediated delivery of FND-protein conjugates was observed by confocal microscopy of co-cultures of HEK and neuroblastoma cells.

5.2. Cell labeling with FNDs

A variety of nanoparticles, such as iron oxide and silica, have been used *in vitro* and *in vivo* for labeling stem cells for extended periods of time (over 30 days). However, conflicting reports on their cytotoxicity or effects on cell differentiation have raised concern for the use of these materials in translational medicine [173]. This issue seems not be present with FNDs, which are widely reported to be non-cytotoxic and highly stable probes for tracking a variety of cell lines including macrophages and stem cells both *in vitro* and *in vivo* [91, 92, 174]. FNDs have also been used to monitor stem cell differentiation, without any observed changes in resulting cell morphology or metabolism [84]. Among the first reports on the use

of FNDs *in vivo*, Mohan *et al*. investigated the long-term tracking of nanoparticle biodistribution in *C. elegans* over multiple generations with no signs of toxicity or stress [175]. FNDs were also administered to mice by weekly intraperitoneal injections at 5 mg/kg and observed for up to 5 months *in vivo* [176]. Compared to control mice, the FND-administered mice exhibited no signs of toxicity after 5 months.

One important subset of research for FND labeling is the long-term tracking of cancer stem cells (CSCs). CSCs represent a small subpopulation of tumor cells that are elusive to chemotherapy treatments due to their quiescence and plasticity which are difficult to detect. Similarly, their mechanisms of tumor propagation are poorly understood. To explain their quiescent behavior and ultimately develop a diagnostic and treatment tool, highly stable fluorescent probes such as FNDs must be used [177]. FND labeling of CSCs facilitated the tracking of stem cell activity for over 20 days. By correlating decreases in fluorescence intensity with the cell division of CSCs, the cell labeling was able to distinguish active from dormant CSCs. Further investigation of FND labeling of CSCs could establish a method of detecting these cells for *in vivo* diagnostics.

Another practical function of FNDs is their use for tracking stem cell. In a recent investigation of FNDs to monitor the progress of a stem cell therapy *in vivo*, Wu *et al*. delivered FND-labeled lung stem cells (LSCs) to mice by intravenous injection and observed stem cell proliferation, differentiation, and engraftment capacity over two weeks [164]. Cell proliferation and differentiation were successfully tracked throughout the healing period, and interestingly, the labeled LSCs were discovered to primarily accumulate in pulmonary tissue as opposed to other organs. Specifically, through combined analysis by fluorescence-activated cell sorting (FACS), fluorescent microscopy, and immunostaining, the tissue-specific location of stem cell engraftment was determined. The LSCs migrated to terminal bronchioles in the lungs of the mice, and furthermore, the treatment successfully regenerated the damaged epithelial lining (Figure 6C). Most recently, FND labeling of mesenchymal stem cells (MSCs) has also been studied *in vivo* in a miniature pig model [178]. Albumin-coated FNDs 100 nm in diameter were used to label MSCs, which were then intravenously injected into miniature pigs., The MSCs distribution *in vivo* was tracked using a combined imaging technique of time-gated fluorescence with confocal microscopy and magnetic modulation. The former method enabled background-free imaging of the cells, and the latter technique of magnetic modulation was utilized to probe the NV^- centers of the FNDs to measure the precise particle count. Overall these methods combined facilitated real-time *in vivo* tracking of accurate numbers of FND particles with respect to their biodistribution. The study found that over 70% of the MSCs accumulated in the terminal bronchioles of the lungs of the pigs. Other studies have shown that magnetic modulation techniques can improve the signal-to-background noise ratio of NV^- FNDs by 100-fold for *in vivo* particle tracking [179].

5.3. MRI contrast agents

Meanwhile FNDs have allowed researchers to conduct single particle or cell tracking experiments that have not been possible with other fluorophores, there is also an abundance of potential clinical applications for NDs as tissue contrast agents in magnetic resonance

imaging (MRI). MRI is the primary medical imaging technique utilized in modern medicine for non-invasive detection and monitoring of soft tissue tumors. In many soft tissues, patients must be administered MRI contrast agents prior to imaging in order to improve the visibility of tissues which emit similar ^{1}H-NMR signals. The most common contrast agents are vehicles for paramagnetic ions such as gadolinium(III) (Gd) and due to their toxicity and inability to accumulate within cells, are only effective for short-term imaging. Thus, there is a need for enhanced or superior contrast agents which will allow radiologists to observe the long-term fate of tumors.

Towards the goal of optimizing contrast-enhanced MRI techniques, paramagnetic contrast agents can be modified with nanomaterials to enhance the relaxivity or rate at which the contrast agent exhibits shortened relaxation times. One factor which defines the relaxivity of such modified contrast agents is the electrostatic forces between paramagnetic ions and water molecules. NDs have recently been identified as one of the most efficient nanomaterials to date for enhancing contrast agents. The highly ordered yet tunable electrostatic interactions unique to NDs that occur due to their faceted crystal lattice structure and diverse surface chemistry results in the adsorption of water molecules to certain facets and essentially forms an ND-solvent interface. By conjugating paramagnetic ions to NDs, their relaxivity is improved due to the increased interaction of the ions with water of the solvent phase present on the ND surface. To demonstrate this concept, Gd(III) chelates were chemically conjugated with amino-functionalized NDs by carbodiimide crosslinking to form ND-Gd aggregates [180]. ND-Gd displayed a 10-fold increase in relaxivity with respect to unmodified Gd. ND-Gd was evaluated *in vivo* as a long-term cell tracking agent for xenografted tumors in mice, revealing that cellular uptake and retention of Gd is increased by 300% when delivered by NDs. The biocompatible ND-Gd complexes enabled the observation of tumor growth by MRI for 26 days. Tumor cells labeled with high concentrations of ND-Gd initially provided negative contrast in T_1-weighted images, and as tumor growth and differentiation occurred which resulted in the dilution of ND-Gd concentrations, the signal reversed to display T_1-weighted positive contrast. In fact, this concentration-dependent shift in contrast was further analyzed by relaxation time in comparison to healthy tissue, and from this data a model was developed which was used to predict tumor morphology and cellular architecture at day 26 based on MR images alone. This model, which was verified in this study by comparison with histology, can be used in future studies to monitor growth dynamics and morphological changes during tumor progression [180]. Furthermore, ND-Gd labeling was noted to have no noticeable effect on cell growth or differentiation, and biodistribution studies after 26 days concluded that 95% of ND-Gd remained within the labeled cells throughout the entire duration of the study. Similarly, Hou *et al.* recently showed that NDs are also useful nanocarriers for manganese (Mn^{2+}) ions as dual mode contrast agents [181]. While Gd agents are commonly used in the clinic as T_1 contrast agents with great success, there is frequently a need for dual mode T_1–T_2 contrast agents to accurately image solid tumors. Specifically, amino-functionalized NDs can chelate Mn^{2+} ions forming ND-Mn complexes, which displayed transverse and longitudinal relaxivity that significantly enhanced the efficacy of Mn as a T_1–T_2 weighted dual contrast agent. ND-Mn was administered *in vivo* by IV injection to mice with liver cancer xenografts. ND-Mn provided superior T_1 and T_2 weighted contrast when compared

with other clinically available dual mode contrast agents, in MRI detection of hepatic tumors, while reducing the cytotoxic effects of Mn^{2+} ions. Serum levels of Mn^{2+} measured at 12 hours post-administration of ND-Mn were approximately 30 ppb and undetectable at earlier time points. Meanwhile, administration of $MnCl_2$ resulted in serum levels of 108 ppb after 1 hour.

Despite the success of NDs for delivery of contrast agents *in vivo*, cytotoxicity of Gd and Mn chelates raises concern for potential use in long-term cell tracking by MR imaging. Recent study has shown that the paramagnetic impurities including nitrogen vacancies and unpaired electrons in the sp^2 shell of NDs can provide a source of contrast signal for MR imaging with high spatial resolution [182]. Through a mechanism known as the Overhauser effect, a low-powered magnetic field transfers spin polarization from the NDs' paramagnetic impurities to ^1H nuclei of the water surrounding the NDs. By *in situ* hyperpolarization, a concentration-dependent and switchable background-free contrast was demonstrated by both untreated and oxidized HPHT NDs and detonation NDs. Using 18 nm in diameter HPHT NDs, Overhauser-enhanced MR imaging (OMRI) was found to be suitable for *in vivo* imaging applications at an ND concentration of 1 mg/mL. Interestingly, oxidation of NDs resulted in increased T_1 relativity and reduced Overhauser enhancement, since oxidation removes the paramagnetic impurities on the ND surface. Overall, OMRI with NDs is a promising technology for future theranostic applications in the clinic, but further studies are necessary to confirm the long-term tracking capabilities of NDs in *in vivo* models.

6. Multimodal applications of NDs

As discussed in the previous sections, one of the most significant advantages of NDs is that different strategies can be combined together simply by making use of their versatile and multifunctional properties. For instance, their drug delivery features can be integrated with their inherent ability to emit fluorescence in order to track the cell internalization of a drug. Similarly, the presence of selected functional groups on the NDs surface can be used both to enhance the mechanical properties of polymeric scaffolds and to modulate the release of growth factors necessary to accelerate the process of tissue regeneration. This great versatility, which cannot be accomplished with any other existing nanoparticles, allows the design of theranostic approaches that can address multiple challenges at the same time overcoming current issues with existing therapies. The bright future of this very nascent trend, which has only emerged in the past year, will be highlighted by a discussion of two preclinical and one clinical study that each utilizes the combined properties of NDs as a bioimaging, delivery, and tissue engineering platform.

Petrakova *et al.* investigated the combination of NDs for DNA delivery and bioimaging probes, and in this 2016 report, the researchers discovered that the by monitoring the change of luminescence of NV^- centers with respect to time in carboxylated NDs, they could image the subcellular DNA transfection in real time. An extraordinary trend was also observed in which the local charge state within the vicinity of the particle directly impacts the luminescence intensity of the NV^- centers, and thus the adsorption or desorption of DNA from the FNDs could be tracked with unprecedented precision by direct optical measurement of the FND luminescence [174]. To demonstrate this proof of concept, the

group formed cationic FND vectors by adsorbing PEI to the surfaces of carboxylated FNDs, to which plasmid DNA was physically adsorbed. Upon delivery to macrophages *in vitro*, PEI-modified FND complexes were tracked in real time with fluorescent microscopy, and the release of plasmid DNA from the FNDs was also tracked by monitoring changes in the luminescence. Not only can this platform be used to monitor the release of DNA from the cationic FND carriers after cellular internalization, but it can also be used to optimize the loading and release kinetics of DNA and the long term stability of the vector even after administration in a biological target (Figure 7A). Further development of this concept toward a therapeutic platform could include the conjugation of targeting ligands to FNDs as discussed previously. For instance, the conjugation of actin or mitochondria antibodies to FNDs has enabled subcellular targeting of these organelles *in vitro*, monitored in real time by fluorescence microscopy [183].

The first demonstration of a combined tissue engineering and bioimaging concept using NDs has also been reported in the previous year and describes a new approach towards *in vivo* tracking of tissue scaffold degradation by sub-dermal fluorescent imaging of composite FND-PCL scaffolds over extended time points. Fox *et al*. demonstrated that FNDs could be incorporated into PCL scaffolds to improve the hydrophilicity and wettability of the scaffold as well as allow direct visualization of the biomaterial *in vivo* to monitor its degradation rate [184]. FND-modified PCL scaffolds were implanted subdermally in pigs, and a customized confocal microscope enabled non-invasive fluorescent imaging of the PCL implant *in vivo* with the ability to track the long-term degradation of the PCL scaffold (Figure 7B).

In addition to the combined strategies previously discussed, a recently initiated Phase I clinical trial is currently being conducted by the research group of Dean Ho to study the multifunctional application of NDs in tissue scaffolding and biomolecule delivery with the goal of improving current treatments offered for root canal therapy. This treatment most commonly involves the removal of infected dental pulp and filling the endodontic cavity with gutta-percha polymer. However, post-operative complications can include re-infection of the site of debriding and poor retention of gutta-percha within the endodontic cavity. This clinical study is aimed to address both of these issues by, incorporating antibiotic-loaded carboxylated NDs into gutta-percha to effectively enhance both the antibacterial and mechanical properties of the polymeric mixture simultaneously. The clinical study, which is notably the first ever clinical study involving NDs, is currently underway to evaluate the therapeutic benefits of ND-modified gutta-percha (NDGP) and determine the efficacy of NDs both as a nanofiller and as a carrier for amoxicillin. As reported by Lee *et al*. in the preclinical study carboxylated NDs were non-covalently linked with amoxicillin before addition of ND-AMC complexes into gutta-percha polymer at concentrations of 5 – 10 wt% ND. The addition of NDs at 5 to 10 wt% to the polymeric mixture resulted in a respective 49% and 247% increase in elastic modulus and a respective 74% and 171% increase in tensile strength [128]. NDGP containing 5 wt% NDs was selected as the optimal concentration used for the ongoing clinical trial (Figure 7C).

7. Conclusion and outlook

In the last decade, nanodiamonds have emerged as a promising platform that enables the design of innovative strategies in several areas of research ranging from drug delivery to bioimaging. Several key factors have played a major role in determining their success in the biomedical field. For instance, the discovery of new techniques of production and purification have allowed the fabrication of NDs with a more defined size and surface chemistry which are both essential requirements for any further development and use in a clinical setting. Their inherent biocompatibility and rapid cellular internalization, as well as their excellent fluorescent properties, represent the rationale behind their well-known use as cell tracking devices. Based on these unique features, researchers have envisioned the possible use of NDs not only as carriers for chemotherapeutic agents but as versatile nanocarriers with multiple applications including bioimaging and selective targeting.

Despite this set of unique advantages, the development of ND-based therapies in the clinic is still hindered by a series of challenges that need to be addressed. One of the main concerns is whether or not NDs can be used in the clinic due to their potential toxicity. The majority of the results obtained from experiments carried out *in vitro* are inconclusive as they are generally based on 2D models that cannot adequately mimic the complexity of *in vivo* settings. On the contrary, the design of 3D cell culture models can be an important strategy to overcome this issue and better predict the biological response *in vivo* [185].

Regarding instead the NDs' fate once administered *in vivo*, Moore *et al.* have recently reported for the first time the long-term effects of DND administration to non-human primates over the course of 6 months [96]. DNDs, which were administered in monthly bolus injections, did not affect the organ functions of non-human primates at moderate or high concentrations (15 mg/kg and 25 mg/kg, respectively). These promising results are possibly the most comprehensive biocompatibility assessment of NDs to date, although this study was based on DNDs, which have limited applications for drug delivery applications due to their high tendency of forming aggregates. On the contrary, NDs coated with polymers or inorganic materials have greater stability and display improved features compared to DNDs but limited evidence has been gathered regarding their safety. For this reason, more studies should be carried out investigating the *in vivo* biodistribution, as well as the possible toxicity induced by the inclusion of a coating on the NDs' surface. Furthermore, a similar assessment regarding the biocompatibility *in vivo* of FNDs should be carried out to validate their safety prior to their use in clinical applications, as only a limited number of studies are investigating the biodistribution of FNDs after administration in animal models [176].

Finally, the use of FNDs as tracking devices in clinical settings is still limited by technological obstacles associated with their production. For instance, there are three main issues that needs to be address such as the high cost associated with their production, the low brightness for FNDs with size smaller than 100 nm and their instability in a biological environment. To resolve these challenges, recent efforts have been made to design new synthetic techniques based on irradiation with 2–3 MeV electrons that allow the production

of FNDs in large scale (hundred grams per batch) with size less than 100 nm and optimized brightness [186].

Future developments in the use of NDs in cancer therapy will consist of the design of new strategies that aim to combine the bioimaging features together with surface modifications to improve existing therapies and obtain more selective results in the treatment of tumors limiting the damage to healthy tissue. For instance, examples in this direction are the use of peptide-targeted FNDs for photoacoustic imaging of breast cancer [187] or the synergistic drug delivery of chemotherapeutic agents combined with photodynamic therapy to produce oxygen species and enhance tumor therapy [188].

As well as providing targeted delivery platforms, the advantageous properties of NDs will be utilized in tissue engineering and prosthetic devices in the near future in clinical trials. Recent advancements in neural prosthetics include the 2016 European Conformity (CE) approval of the Iris® II retinal implant developed by Pixium Vision. In September of 2016, this device was implanted into a patient with retinisis pigmentosa, and this sub-retinal and intra-ocular implant consisting of 150 electrodes within a conductive polymeric film successfully restored vision to the patient who had been fully blind for years. A larger scale clinical trial is underway in Europe (NCT02670980), and this exciting milestone in neural prosthetics will lead tissue engineers to develop even more effective and less expensive retinal implants. In fact, preclinical models of carbon nanostructured retinal prosthetics have already emerged within the past two years that feature patterned microarrays of electrodes. Both *in vitro* and *in vivo* studies have evaluated the efficacy of using ND films to create a flexible 3D implant with 25x25 microarrays of electrodes, which is over a 5-fold improvement in image resolution compared to the Iris® II [189]. Retinal prosthetics fabricated with patterned microarrays of ND electrodes can therefore provide higher resolution images to patients, and several studies have already shown the possibility of stimulating dorsal root ganglia *in vivo* with nitrogen-doped ND films [190]. In addition to their functionality that can be utilized to fabricate conductive microstructures, the long term stability and bioinert properties exhibited by NDs have undoubtedly garnered widespread interest of this carbon nanomaterial for use as a composite implant material for enhanced root canal therapy in the first clinical study with NDs which commenced in March of 2017 (NCT02698163). Further studies to explore the potential of NDs as both cell substrates and as long term biosensors, following a similar concept as theranostic ND platforms for drug delivery, will demonstrate the versatility and high impact of this nanomaterial in regenerative medicine.

Acknowledgments

A.P. acknowledges an investigator grant provided by NIH P20 cobre and State of Kansas funding support for umbilical cord matrix.

References

1. Vul, AY., et al. Nanodiamond. The Royal Society of Chemistry; 2014. CHAPTER 2 Detonation Nanodiamonds: Synthesis, Properties and Applications; p. 27-48.
2. Wang X, et al. Epirubicin-Adsorbed Nanodiamonds Kill Chemoresistant Hepatic Cancer Stem Cells. ACS Nano. 2014; 8(12):12151–12166. [PubMed: 25437772]

3. Chow EK, et al. Nanodiamond therapeutic delivery agents mediate enhanced chemoresistant tumor treatment. Science translational medicine. 2011; 3(73):73ra21–73ra21.
4. Ma, X-w, Zhao, Y-l, Liang, X-j. Nanodiamond delivery circumvents tumor resistance to doxorubicin. Acta Pharmacol Sin. 2011; 32(5):543–544. [PubMed: 21532613]
5. Zhang XQ, et al. Polymer-functionalized nanodiamond platforms as vehicles for gene delivery. ACS nano. 2009; 3(9):2609–2616. [PubMed: 19719152]
6. Perevedentseva E, et al. Nanodiamond internalization in cells and the cell uptake mechanism. Journal of Nanoparticle Research. 2013; 15(8):1834.
7. Lin CL, et al. Protein Attachment on Nanodiamonds. The Journal of Physical Chemistry A. 2015; 119(28):7704–7711. [PubMed: 25815400]
8. Moore L, et al. Multi-protein Delivery by Nanodiamonds Promotes Bone Formation. Journal of Dental Research. 2013; 92(11):976–981. [PubMed: 24045646]
9. Kaur R, et al. Lysine-functionalized nanodiamonds: synthesis, physiochemical characterization, and nucleic acid binding studies. International Journal of Nanomedicine. 2012; 7:3851–3866. [PubMed: 22904623]
10. Grausova L, et al. Nanodiamond as promising material for bone tissue engineering. J Nanosci Nanotechnol. 2009; 9(6):3524–34. [PubMed: 19504878]
11. Chen, YC., et al. Diamond-Based Materials for Biomedical Applications. Woodhead Publishing; 2013. 7 - Ultrananocrystalline diamond (UNCD) for neural applications A2 - Narayan, R; p. 171-185.
12. Hikov T, et al. Studying the influence of nanodiamonds over the elasticity of polymer/nanodiamond composites for biomedical application. Journal of Physics: Conference Series. 2014; 558(1):012060.
13. Catledge SA, Thomas V, Vohra YK. Nanostructured diamond coatings for orthopaedic applications. Woodhead publishing series in biomaterials. 2013; 2013:105–150. [PubMed: 25285213]
14. Zhu Y, et al. The Biocompatibility of Nanodiamonds and Their Application in Drug Delivery Systems. Theranostics. 2012; 2(3):302–312. [PubMed: 22509196]
15. Yuen Yung H, Chia-Liang C, Huan-Cheng C. Nanodiamonds for optical bioimaging. Journal of Physics D: Applied Physics. 2010; 43(37):374021.
16. Danilenko VV. On the history of the discovery of nanodiamond synthesis. Physics of the Solid State. 2004; 46(4):595–599.
17. Krueger A, Lang D. Functionality is Key: Recent Progress in the Surface Modification of Nanodiamond. Advanced Functional Materials. 2012; 22(5):890–906.
18. Viecelli JA, Glosli JN. Carbon cluster coagulation and fragmentation kinetics in shocked hydrocarbons. The Journal of Chemical Physics. 2002; 117(24):11352–11358.
19. Barnard AS. Self-assembly in nanodiamond agglutinates. Journal of Materials Chemistry. 2008; 18(34):4038–4041.
20. Yu Dolmatov V. Detonation synthesis ultradispersed diamonds: properties and applications. Russian Chemical Reviews. 2001; 70(7):607–626.
21. Petrov I, et al. Detonation nanodiamonds simultaneously purified and modified by gas treatment. Diamond and Related Materials. 2007; 16(12):2098–2103.
22. Krüger A, et al. Unusually tight aggregation in detonation nanodiamond: Identification and disintegration. Carbon. 2005; 43(8):1722–1730.
23. Xu X, et al. Effect of sodium oleate adsorption on the colloidal stability and zeta potential of detonation synthesized diamond particles in aqueous solutions. Diamond and Related Materials. 2005; 14(2):206–212.
24. Williams OA, et al. Size-Dependent Reactivity of Diamond Nanoparticles. ACS Nano. 2010; 4(8):4824–4830. [PubMed: 20731457]
25. Neburkova J, Vavra J, Cigler P. Coating nanodiamonds with biocompatible shells for applications in biology and medicine. Current Opinion in Solid State and Materials Science. 2017; 21(1):43–53.

26. Shi Y, et al. Direct surface PEGylation of nanodiamond via RAFT polymerization. Applied Surface Science. 2015; 357(Part B):2147–2153.
27. Zhao L, et al. Chromatographic Separation of Highly Soluble Diamond Nanoparticles Prepared by Polyglycerol Grafting. Angewandte Chemie International Edition. 2011; 50(6):1388–1392. [PubMed: 21290519]
28. Morita Y, et al. A facile and scalable process for size-controllable separation of nanodiamond particles as small as 4 nm. Small. 2008; 4(12):2154–7. [PubMed: 18989864]
29. Ozawa M, et al. Preparation and Behavior of Brownish, Clear Nanodiamond Colloids. Advanced Materials. 2007; 19(9):1201–1206.
30. Pentecost A, et al. Deaggregation of Nanodiamond Powders Using Salt- and Sugar-Assisted Milling. ACS Applied Materials & Interfaces. 2010; 2(11):3289–3294. [PubMed: 21043470]
31. Turcheniuk K, et al. Salt-Assisted Ultrasonic Deaggregation of Nanodiamond. ACS Applied Materials & Interfaces. 2016; 8(38):25461–25468. [PubMed: 27589086]
32. Mochalin VN, et al. The properties and applications of nanodiamonds. Nat Nano. 2012; 7(1):11–23.
33. Kalbacova M, et al. Nanoscale topography of nanocrystalline diamonds promotes differentiation of osteoblasts. Acta Biomater. 2009; 5(8):3076–85. [PubMed: 19433140]
34. Xing Z, et al. Biological effects of functionalizing copolymer scaffolds with nanodiamond particles. Tissue Eng Part A. 2013; 19(15–16):1783–91. [PubMed: 23574424]
35. Shi B, et al. Fundamentals of ultrananocrystalline diamond (UNCD) thin films as biomaterials for developmental biology: Embryonic fibroblasts growth on the surface of (UNCD) films. Diamond and Related Materials. 2009; 18(2–3):596–600.
36. Auciello O, Sumant AV. Status review of the science and technology of ultrananocrystalline diamond (UNCD) films and application to multifunctional devices. Diamond and Related Materials. 2010; 19(7–9):699–718.
37. Fang L, Ohfuji H, Irifune T. A Novel Technique for the Synthesis of Nanodiamond Powder. Journal of Nanomaterials. 2013; 2013:4.
38. Stehlik S, et al. Size and Purity Control of HPHT Nanodiamonds down to 1 nm. The Journal of Physical Chemistry C. 2015; 119(49):27708–27720.
39. Peristyy AA, et al. Diamond based adsorbents and their application in chromatography. Journal of Chromatography A. 2014; 1357:68–86. [PubMed: 24999070]
40. Michaelson S, et al. Hydrogen concentration and bonding configuration in polycrystalline diamond films: From micro-to nanometric grain size. Journal of Applied Physics. 2007; 102(11):113516.
41. Rehor I, et al. Fluorescent Nanodiamonds Embedded in Biocompatible Translucent Shells. Small (Weinheim an der Bergstrasse, Germany). 2014; 10(6):1106–1115.
42. Nee CH, et al. Direct synthesis of nanodiamonds by femtosecond laser irradiation of ethanol. Scientific Reports. 2016; 6:33966. [PubMed: 27659184]
43. Yang L, et al. Growth of diamond nanocrystals by pulsed laser ablation of graphite in liquid. Diamond and Related Materials. 2007; 16(4–7):725–729.
44. Zousman, B., Levinson, O. Nanodiamond. The Royal Society of Chemistry; 2014. Chapter 5 Pure Nanodiamonds Produced by Laser-assisted Technique; p. 112-127.
45. Nee CH, et al. Direct synthesis of nanodiamonds by femtosecond laser irradiation of ethanol. Sci Rep. 2016; 6:33966. [PubMed: 27659184]
46. Mitev D, et al. Surface peculiarities of detonation nanodiamonds in dependence of fabrication and purification methods. Diamond and related materials. 2007; 16(4):776–780.
47. Anikeev VI V, Zaikovskii I. Treatment of detonation carbon in supercritical water. Russian Journal of Applied Chemistry. 2010; 83(7):1202–1208.
48. Shenderova O, et al. Surface chemistry and properties of ozone-purified detonation nanodiamonds. The Journal of Physical Chemistry C. 2011; 115(20):9827–9837.
49. Osswald S, et al. Control of sp2/sp3 carbon ratio and surface chemistry of nanodiamond powders by selective oxidation in air. J Am Chem Soc. 2006; 128(35):11635–42. [PubMed: 16939289]
50. Adach K, Fijalkowski M, Skolimowski J. Antioxidant effect of hydroxylated diamond nanoparticles measured in soybean oil. Fullerenes, Nanotubes and Carbon Nanostructures. 2015

51. Martín R, et al. General Strategy for High-Density Covalent Functionalization of Diamond Nanoparticles Using Fenton Chemistry. Chemistry of Materials. 2009; 21(19):4505–4514.
52. Krueger A, et al. Biotinylated nanodiamond: simple and efficient functionalization of detonation diamond. Langmuir. 2008; 24(8):4200–4204. [PubMed: 18312008]
53. Zhao F, et al. Carbon Fiber Grafted with Nanodiamond: Preparation and Characterization. Journal of Nanoscience and Nanotechnology. 2015; 15(8):5807–5815. [PubMed: 26369155]
54. Zheng WW, et al. Organic functionalization of ultradispersed nanodiamond: synthesis and applications. Journal of Materials Chemistry. 2009; 19(44):8432–8441.
55. Liang Y, Ozawa M, Krueger A. A general procedure to functionalize agglomerating nanoparticles demonstrated on nanodiamond. ACS Nano. 2009; 3(8):2288–96. [PubMed: 19601635]
56. Yeap WS, Chen S, Loh KP. Detonation Nanodiamond: An Organic Platform for the Suzuki Coupling of Organic Molecules. Langmuir. 2009; 25(1):185–191. [PubMed: 19049362]
57. Zhong YL, Loh KP. The chemistry of C-H bond activation on diamond. Chem Asian J. 2010; 5(7): 1532–40. [PubMed: 20419726]
58. Su S, et al. Hydrogen-terminated detonation nanodiamond: Impedance spectroscopy and thermal stability studies. Journal of Applied Physics. 2013; 113(2):023707.
59. Panich AM, et al. Structure and Bonding in Fluorinated Nanodiamond. The Journal of Physical Chemistry C. 2010; 114(2):774–782.
60. Lisichkin GV, et al. Photochemical chlorination of nanodiamond and interaction of its modified surface with C-nucleophiles. Russian Chemical Bulletin. 2006; 55(12):2212–2219.
61. Korobov MV, et al. Aggregate structure of “single-nano buckydiamond” in gel and dried powder by differential scanning calorimetry and nitrogen adsorption. Diamond and Related Materials. 2010; 19(5–6):665–671.
62. Mochalin VN, Gogotsi Y. Wet Chemistry Route to Hydrophobic Blue Fluorescent Nanodiamond. Journal of the American Chemical Society. 2009; 131(13):4594–4595. [PubMed: 19290627]
63. Koch H, et al. Plasma amination of ultrananocrystalline diamond/amorphous carbon composite films for the attachment of biomolecules. Diamond and Related Materials. 2011; 20(2):254–258.
64. Krueger A, et al. Deagglomeration and functionalisation of detonation diamond. physica status solidi (a). 2007; 204(9):2881–2887.
65. Kruger A, et al. Surface functionalisation of detonation diamond suitable for biological applications. Journal of Materials Chemistry. 2006; 16(24):2322–2328.
66. Purtov KV, et al. Nanodiamonds as Carriers for Address Delivery of Biologically Active Substances. Nanoscale Res Lett. 2010; 5(3):631–636. [PubMed: 20672079]
67. Zhao L, et al. Polyglycerol-functionalized nanodiamond as a platform for gene delivery: Derivatization, characterization, and hybridization with DNA. Beilstein journal of organic chemistry. 2014; 10(1):707–713. [PubMed: 24778723]
68. Huang LCL, Chang HC. Adsorption and Immobilization of Cytochrome c on Nanodiamonds. Langmuir. 2004; 20(14):5879–5884. [PubMed: 16459604]
69. Neburkova J, Vavra J, Cigler P. Coating nanodiamonds with biocompatible shells for applications in biology and medicine. Current Opinion in Solid State and Materials Science.
70. Zhang X, et al. A comparative study of cellular uptake and cytotoxicity of multi-walled carbon nanotubes, graphene oxide, and nanodiamond. Toxicology Research. 2012; 1(1):62–68.
71. Solarska-Sciuk K, et al. Cellular redox homeostasis in endothelial cells treated with nonmodified and Fenton-modified nanodiamond powders. Biotechnol Appl Biochem. 2014; 61(5):593–602. [PubMed: 24433188]
72. Solarska-Sciuk K, et al. Stimulation of production of reactive oxygen and nitrogen species in endothelial cells by unmodified and Fenton-modified ultradisperse detonation diamond. Biotechnol Appl Biochem. 2013; 60(2):259–65. [PubMed: 23586587]
73. Solarska K, et al. Induction of apoptosis in human endothelial cells by nanodiamond particles. J Nanosci Nanotechnol. 2012; 12(6):5117–21. [PubMed: 22905588]
74. Wierzbicki M, et al. Carbon nanoparticles downregulate expression of basic fibroblast growth factor in the heart during embryogenesis. Int J Nanomedicine. 2013; 8:3427–35. [PubMed: 24039425]

75. Wierzbicki M, et al. Comparison of anti-angiogenic properties of pristine carbon nanoparticles. Nanoscale Res Lett. 2013; 8(1):195. [PubMed: 23618362]
76. Keremidarska M, et al. Comparative study of cytotoxicity of detonation nanodiamond particles with an osteosarcoma cell line and primary mesenchymal stem cells. Biotechnol Biotechnol Equip. 2014; 28(4):733–739. [PubMed: 26019557]
77. Paget V, et al. Carboxylated nanodiamonds are neither cytotoxic nor genotoxic on liver, kidney, intestine and lung human cell lines. Nanotoxicology. 2014; 8(Suppl 1):46–56. [PubMed: 24266793]
78. Xing Y, et al. DNA Damage in Embryonic Stem Cells Caused by Nanodiamonds. ACS Nano. 2011; 5(3):2376–2384. [PubMed: 21370893]
79. Marcon L, et al. Cellular and in vivo toxicity of functionalized nanodiamond in Xenopus embryos. Journal of Materials Chemistry. 2010; 20(37):8064–8069.
80. Zhu Y, et al. Nanodiamonds act as Trojan horse for intracellular delivery of metal ions to trigger cytotoxicity. Part Fibre Toxicol. 2015; 12:2. [PubMed: 25651858]
81. Villalba P, et al. Cellular and in vitro toxicity of nanodiamond-polyaniline composites in mammalian and bacterial cell. Materials Science and Engineering: C. 2012; 32(3):594–598.
82. Zhang Q, et al. Fluorescent PLLA-nanodiamond composites for bone tissue engineering. Biomaterials. 2011; 32(1):87–94. [PubMed: 20869765]
83. Liu KK, et al. Endocytic carboxylated nanodiamond for the labeling and tracking of cell division and differentiation in cancer and stem cells. Biomaterials. 2009; 30(26):4249–59. [PubMed: 19500835]
84. Hsu TC, et al. Labeling of neuronal differentiation and neuron cells with biocompatible fluorescent nanodiamonds. Sci Rep. 2014; 4
85. Blaber SP, et al. Effect of Labeling with Iron Oxide Particles or Nanodiamonds on the Functionality of Adipose-Derived Mesenchymal Stem Cells. PLOS ONE. 2013; 8(1):e52997. [PubMed: 23301012]
86. Moore L, et al. Comprehensive Interrogation of the Cellular Response to Fluorescent, Detonation and Functionalized Nanodiamonds. Nanoscale. 2014; 6(20):11712–11721. [PubMed: 25037888]
87. Hsu MH, et al. Directly thiolated modification onto the surface of detonation nanodiamonds. ACS Appl Mater Interfaces. 2014; 6(10):7198–203. [PubMed: 24766528]
88. Zhao L, et al. Polyglycerol-coated nanodiamond as a macrophage-evading platform for selective drug delivery in cancer cells. Biomaterials. 2014; 35(20):5393–406. [PubMed: 24720879]
89. Huang H, et al. Active nanodiamond hydrogels for chemotherapeutic delivery. Nano Lett. 2007; 7(11):3305–14. [PubMed: 17918903]
90. Faklaris O, et al. Photoluminescent Diamond Nanoparticles for Cell Labeling: Study of the Uptake Mechanism in Mammalian Cells. ACS Nano. 2009; 3(12):3955–3962. [PubMed: 19863087]
91. Fang CY, et al. The exocytosis of fluorescent nanodiamond and its use as a long-term cell tracker. Small. 2011; 7(23):3363–70. [PubMed: 21997958]
92. Schrand AM, et al. Temporal and mechanistic tracking of cellular uptake dynamics with novel surface fluorophore-bound nanodiamonds. Nanoscale. 2011; 3(2):435–45. [PubMed: 20877788]
93. Yuan Y, et al. Biodistribution and fate of nanodiamonds in vivo. Diamond and Related Materials. 2009; 18(1):95–100.
94. Zhang X, et al. Biodistribution and toxicity of nanodiamonds in mice after intratracheal instillation. Toxicol Lett. 2010; 198(2):237–43. [PubMed: 20633617]
95. Yuan Y, et al. Pulmonary toxicity and translocation of nanodiamonds in mice. Diamond and Related Materials. 2010; 19(4):291–299.
96. Moore L, et al. Biocompatibility Assessment of Detonation Nanodiamond in Non-Human Primates and Rats Using Histological, Hematologic, and Urine Analysis. ACS Nano. 2016; 10(8):7385–400. [PubMed: 27439019]
97. Cho K, et al. Therapeutic nanoparticles for drug delivery in cancer. Clin Cancer Res. 2008; 14(5): 1310–6. [PubMed: 18316549]
98. Abdullah LN, Chow EKH. Mechanisms of chemoresistance in cancer stem cells. Clinical and Translational Medicine. 2013; 2:3–3. [PubMed: 23369605]

99. Shi J, et al. Cancer nanomedicine: progress, challenges and opportunities. Nat Rev Cancer. 2017; 17(1):20–37. [PubMed: 27834398]
100. Lee JJ, Saiful Yazan L, Che Abdullah CA. A review on current nanomaterials and their drug conjugate for targeted breast cancer treatment. International Journal of Nanomedicine. 2017; 12:2373–2384. [PubMed: 28392694]
101. Hagiwara A, et al. Methotrexate bound to carbon particles used for treating cancers with lymph node metastases in animal experiments and a clinical pilot study. Cancer. 1996; 78(10):2199–209. [PubMed: 8918415]
102. Xu XF, Gu J. The application of carbon nanoparticles in the lymph node biopsy of cN0 papillary thyroid carcinoma: A randomized controlled clinical trial. Asian Journal of Surgery.
103. Liu KK, et al. Covalent linkage of nanodiamond-paclitaxel for drug delivery and cancer therapy. Nanotechnology. 2010; 21(31):315106. [PubMed: 20634575]
104. Chen M, et al. Nanodiamond-mediated delivery of water-insoluble therapeutics. ACS Nano. 2009; 3(7):2016–22. [PubMed: 19534485]
105. Chang LY, Osawa E, Barnard AS. Confirmation of the electrostatic self-assembly of nanodiamonds. Nanoscale. 2011; 3(3):958–962. [PubMed: 21258697]
106. Whitlow J, Pacelli S, Paul A. Polymeric Nanohybrids as a New Class of Therapeutic Biotransporters. Macromolecular Chemistry and Physics. 2016; 217(11):1245–1259.
107. Xiao J, et al. Nanodiamonds-mediated doxorubicin nuclear delivery to inhibit lung metastasis of breast cancer. Biomaterials. 2013; 34(37):9648–56. [PubMed: 24016858]
108. Wang D, et al. PEGylated nanodiamond for chemotherapeutic drug delivery. Diamond and Related Materials. 2013; 36:26–34.
109. Zhang X, et al. PolyPEGylated nanodiamond for intracellular delivery of a chemotherapeutic drug. Polymer Chemistry. 2012; 3(10):2716–2719.
110. Li L, et al. Acetate ions enhance load and stability of doxorubicin onto PEGylated nanodiamond for selective tumor intracellular controlled release and therapy. Integr Biol (Camb). 2016; 8(9): 956–67. [PubMed: 27502159]
111. Moore L, et al. Diamond-Lipid Hybrids Enhance Chemotherapeutic Tolerance and Mediate Tumor Regression. Advanced Materials. 2013; 25(26):3532–3541. [PubMed: 23584895]
112. Prabhakar N, et al. Core-shell designs of photoluminescent nanodiamonds with porous silica coatings for bioimaging and drug delivery II: application. Nanoscale. 2013; 5(9):3713–3722. [PubMed: 23493921]
113. von Haartman E, et al. Core-shell designs of photoluminescent nanodiamonds with porous silica coatings for bioimaging and drug delivery I: fabrication. Journal of Materials Chemistry B. 2013; 1(18):2358–2366.
114. Slegerova J, et al. Designing the nanobiointerface of fluorescent nanodiamonds: highly selective targeting of glioma cancer cells. Nanoscale. 2015; 7(2):415–420. [PubMed: 25132312]
115. Day BW, Stringer BW, Boyd AW. Eph receptors as therapeutic targets in glioblastoma. Br J Cancer. 2014; 111(7):1255–1261. [PubMed: 25144626]
116. Chen X, et al. Fabrication of an EGF modified nanodiamonds-based anti-cancer drug targeted delivery system and drug carrier uptake visualization by 3D Raman microscopy. RSC Adv. 2016; 6(50):44543–44551.
117. Li X, et al. TAT-conjugated nanodiamond for the enhanced delivery of doxorubicin. Journal of Materials Chemistry. 2011; 21(22):7966–7973.
118. Zhang XQ, et al. Multimodal Nanodiamond Drug Delivery Carriers for Selective Targeting, Imaging, and Enhanced Chemotherapeutic Efficacy. Advanced Materials. 2011; 23(41):4770–4775. [PubMed: 21932280]
119. Chan MS, et al. Cancer-Cell-Specific Mitochondria-Targeted Drug Delivery by Dual-Ligand-Functionalized Nanodiamonds Circumvent Drug Resistance. ACS Applied Materials & Interfaces. 2017; 9(13):11780–11789. [PubMed: 28291330]
120. Alhaddad A, et al. Nanodiamond as a vector for siRNA delivery to Ewing sarcoma cells. Small. 2011; 7(21):3087–95. [PubMed: 21913326]

121. Chen M, et al. Nanodiamond Vectors Functionalized with Polyethylenimine for siRNA Delivery. The Journal of Physical Chemistry Letters. 2010; 1(21):3167–3171.

122. Alwani S, et al. Lysine-functionalized nanodiamonds as gene carriers: development of stable colloidal dispersion for in vitro cellular uptake studies and siRNA delivery application. Int J Nanomedicine. 2016; 11:687–702. [PubMed: 26929623]

123. Zhao L, et al. Polyglycerol-functionalized nanodiamond as a platform for gene delivery: Derivatization, characterization, and hybridization with DNA. Beilstein J Org Chem. 2014; 10:707–13. [PubMed: 24778723]

124. Cui C, et al. RGDS covalently surfaced nanodiamond as a tumor targeting carrier of VEGF-siRNA: synthesis, characterization and bioassay. Journal of Materials Chemistry B. 2015; 3(48): 9260–9268.

125. Bi Y, et al. Gene-silencing effects of anti-survivin siRNA delivered by RGDV-functionalized nanodiamond carrier in the breast carcinoma cell line MCF-7. Int J Nanomedicine. 2016; 11:5771–5787. [PubMed: 27853365]

126. Bailie GR, Neal D. Vancomycin ototoxicity and nephrotoxicity. A review. Med Toxicol Adverse Drug Exp. 1988; 3(5):376–86. [PubMed: 3057327]

127. Giammarco J, et al. The adsorption of tetracycline and vancomycin onto nanodiamond with controlled release. J Colloid Interface Sci. 2016; 468:253–61. [PubMed: 26852349]

128. Lee DK, et al. Nanodiamond–Gutta Percha Composite Biomaterials for Root Canal Therapy. ACS Nano. 2015; 9(11):11490–11501. [PubMed: 26452304]

129. Suliman S, et al. Release and bioactivity of bone morphogenetic protein-2 are affected by scaffold binding techniques in vitro and in vivo. J Control Release. 2015; 197:148–57. [PubMed: 25445698]

130. Pacelli S, et al. Nanodiamond-based injectable hydrogel for sustained growth factor release: preparation, characterization and in vitro analysis. Acta Biomaterialia.

131. Shimkunas RA, et al. Nanodiamond-insulin complexes as pH-dependent protein delivery vehicles. Biomaterials. 2009; 30(29):5720–8. [PubMed: 19635632]

132. Moore L, et al. Multi-protein delivery by nanodiamonds promotes bone formation. J Dent Res. 2013; 92(11):976–81. [PubMed: 24045646]

133. Al-Juffali N, et al. S138 Nanodiamond Delivery Of Vascular Endothelial Growth Factor Promotes Fetal Lung Development In A Rat Model Of Congenital Diaphragmatic Hernia. Thorax. 2014; 69(Suppl 2):A73–A74.

134. Vacanti JP, Langer R. Tissue engineering: the design and fabrication of living replacement devices for surgical reconstruction and transplantation. Lancet. 1999; 354(Suppl 1):Si32–4. [PubMed: 10437854]

135. Hristova K, et al. Improved interaction of osteoblast-like cells with apatite-nanodiamond coatings depends on fibronectin. J Mater Sci Mater Med. 2011; 22(8):1891–900. [PubMed: 21706219]

136. Bacakova L, et al. Adhesion and Growth of Human Osteoblast-Like Cell in Cultures on Nanocomposite Carbon-Based Materials. Nanoscience and Nanotechnology Letters. 2011; 3(1): 99–109.

137. Grausova L, et al. Enhanced Growth and Osteogenic Differentiation of Human Osteoblast-Like Cells on Boron-Doped Nanocrystalline Diamond Thin Films. PLOS ONE. 2011; 6(6):e20943. [PubMed: 21695172]

138. Keremidarska M, et al. Effect of nanodiamond modification of siloxane surfaces on stem cell behaviour. Journal of Physics: Conference Series. 2014; 558(1):012056.

139. Bergkvist M, Carlsson J, Oscarsson S. Surface-dependent conformations of human plasma fibronectin adsorbed to silica, mica, and hydrophobic surfaces, studied with use of Atomic Force Microscopy. J Biomed Mater Res A. 2003; 64(2):349–56. [PubMed: 12522822]

140. Yassin MA, et al. A Copolymer Scaffold Functionalized with Nanodiamond Particles Enhances Osteogenic Metabolic Activity and Bone Regeneration. Macromol Biosci. 2017

141. Thalhammer A, et al. The use of nanodiamond monolayer coatings to promote the formation of functional neuronal networks. Biomaterials. 2010; 31(8):2097–2104. [PubMed: 20035997]

142. Cellot G, et al. Carbon nanotubes might improve neuronal performance by favouring electrical shortcuts. Nat Nano. 2009; 4(2):126–133.

143. Edgington RJ, et al. Patterned neuronal networks using nanodiamonds and the effect of varying nanodiamond properties on neuronal adhesion and outgrowth. J Neural Eng. 2013; 10(5):056022. [PubMed: 24045617]

144. Hopper AP, et al. Amine functionalized nanodiamond promotes cellular adhesion, proliferation and neurite outgrowth. Biomed Mater. 2014; 9(4):045009. [PubMed: 25029630]

145. Taylor AC, et al. Biocompatibility of nanostructured boron doped diamond for the attachment and proliferation of human neural stem cells. J Neural Eng. 2015; 12(6):066016. [PubMed: 26468733]

146. Specht CG, et al. Ordered growth of neurons on diamond. Biomaterials. 2004; 25(18):4073–4078. [PubMed: 15046898]

147. Revell PA. The combined role of wear particles, macrophages and lymphocytes in the loosening of total joint prostheses. J R Soc Interface. 2008; 5(28):1263–78. [PubMed: 18647740]

148. Catledge SA, et al. Improved adhesion of ultra-hard carbon films on cobalt–chromium orthopaedic implant alloy. Journal of materials science Materials in medicine. 2011; 22(2):307–316. [PubMed: 21221739]

149. Lappalainen R, et al. Reduction of wear in total hip replacement prostheses by amorphous diamond coatings. J Biomed Mater Res B Appl Biomater. 2003; 66(1):410–3. [PubMed: 12808601]

150. Papo MJ, et al. Mechanical wear behavior of nanocrystalline and multilayer diamond coatings on temporomandibular joint implants. J Mater Sci Mater Med. 2004; 15(7):773–7. [PubMed: 15387413]

151. Xie Y, et al. Improving the long-term stability of Ti6Al4V abutment screw by coating micro/nano-crystalline diamond films. J Mech Behav Biomed Mater. 2016; 63:174–82. [PubMed: 27393893]

152. Chowdhury S, et al. Synthesis and Mechanical Wear Studies of Ultra Smooth Nanostructured Diamond (USND) Coatings Deposited by Microwave Plasma Chemical Vapor Deposition with He/H(2)/CH(4)/N(2) Mixtures. Diamond and related materials. 2008; 17(4–5):419–427. [PubMed: 19112519]

153. Gutensohn K, et al. In Vitro Analyses of Diamond-like Carbon Coated Stents: Reduction of Metal Ion Release, Platelet Activation, and Thrombogenicity. Thrombosis Research. 2000; 99(6):577–585. [PubMed: 10974344]

154. Thomas V, et al. In vitro studies on the effect of particle size on macrophage responses to nanodiamond wear debris. Acta Biomater. 2012; 8(5):1939–47. [PubMed: 22342422]

155. Rupprecht S, et al. Examination of the bone-metal interface of titanium implants coated by the microwave plasma chemical vapor deposition method. Int J Oral Maxillofac Implants. 2002; 17(6):778–85. [PubMed: 12507236]

156. Salaam AD, Dean D. Electrospun Polycaprolactone-Nanodiamond Composite Scaffolds for Bone Tissue Engineering. 2010; (43925):367–370.

157. Wang Z, et al. Mechanical reinforcement of electrospun water-soluble polymer nanofibers using nanodiamonds. Polymer Composites. 2013; 34(10):1735–1744.

158. Brady MA, et al. Development of Composite Poly(Lactide-<I>co</I>-Glycolide)-Nanodiamond Scaffolds for Bone Cell Growth. Journal of Nanoscience and Nanotechnology. 2015; 15(2):1060–1069. [PubMed: 26353613]

159. Mahdavi M, et al. Electrospinning of Nanodiamond-Modified Polysaccharide Nanofibers with Physico-Mechanical Properties Close to Natural Skins. Mar Drugs. 2016; 14(7)

160. Mochalin VN, et al. Covalent Incorporation of Aminated Nanodiamond into an Epoxy Polymer Network. ACS Nano. 2011; 5(9):7494–7502. [PubMed: 21830823]

161. Zhang F, et al. A Novel High Mechanical Property PLGA Composite Matrix Loaded with Nanodiamond-Phospholipid Compound for Bone Tissue Engineering. ACS Appl Mater Interfaces. 2016; 8(2):1087–97. [PubMed: 26646188]

162. Suliman S, et al. Nanodiamond modified copolymer scaffolds affects tumour progression of early neoplastic oral keratinocytes. Biomaterials. 2016; 95:11–21. [PubMed: 27108402]

163. Schimke MM, et al. Biofunctionalization of scaffold material with nano-scaled diamond particles physisorbed with angiogenic factors enhances vessel growth after implantation. Nanomedicine. 2016; 12(3):823–33. [PubMed: 26654993]

164. Wu TJ, et al. Tracking the engraftment and regenerative capabilities of transplanted lung stem cells using fluorescent nanodiamonds. Nat Nano. 2013; 8(9):682–689.
165. Tisler J, et al. Fluorescence and Spin Properties of Defects in Single Digit Nanodiamonds. ACS Nano. 2009; 3(7):1959–1965. [PubMed: 21452865]
166. Fu CC, et al. Characterization and application of single fluorescent nanodiamonds as cellular biomarkers. Proceedings of the National Academy of Sciences. 2007; 104(3):727–732.
167. Jaqaman K, et al. Robust single-particle tracking in live-cell time-lapse sequences. Nat Meth. 2008; 5(8):695–702.
168. Haziza S, et al. Fluorescent nanodiamond tracking reveals intraneuronal transport abnormalities induced by brain-disease-related genetic risk factors. Nat Nanotechnol. 2016
169. Liu W, et al. 3D Single-Molecule Imaging of Transmembrane Signaling by Targeting Nanodiamonds. Advanced Functional Materials. 2016; 26(3):365–375.
170. Sotoma S, et al. Selective Labeling of Proteins on Living Cell Membranes Using Fluorescent Nanodiamond Probes. Nanomaterials. 2016; 6(4):56.
171. Weng MF, et al. Fluorescent nanodiamonds for specifically targeted bioimaging: Application to the interaction of transferrin with transferrin receptor. Diamond and Related Materials. 2009; 18(2–3):587–591.
172. Epperla CP, et al. Nanodiamond-Mediated Intercellular Transport of Proteins through Membrane Tunneling Nanotubes. Small. 2015; 11(45):6097–6105. [PubMed: 26479149]
173. El-Sadik AO, El-Ansary A, Sabry SM. Nanoparticle-labeled stem cells: a novel therapeutic vehicle. Clinical pharmacology: advances and applications. 2010; 2:9–16. [PubMed: 22291483]
174. Petrakova V, et al. Imaging of transfection and intracellular release of intact, non-labeled DNA using fluorescent nanodiamonds. Nanoscale. 2016; 8(23):12002–12. [PubMed: 27240633]
175. Mohan N, et al. In Vivo Imaging and Toxicity Assessments of Fluorescent Nanodiamonds in Caenorhabditis elegans. Nano Letters. 2010; 10(9):3692–3699. [PubMed: 20677785]
176. Vaijayanthimala V, et al. The long-term stability and biocompatibility of fluorescent nanodiamond as an in vivo contrast agent. Biomaterials. 2012; 33(31):7794–802. [PubMed: 22863379]
177. Li L, Bhatia R. Stem cell quiescence. Clin Cancer Res. 2011; 17(15):4936–41. [PubMed: 21593194]
178. Su LJ, et al. Fluorescent nanodiamonds enable quantitative tracking of human mesenchymal stem cells in miniature pigs. Scientific Reports. 2017; 7:45607. [PubMed: 28358111]
179. Sarkar SK, et al. Wide-field in vivo background free imaging by selective magnetic modulation of nanodiamond fluorescence. Biomedical Optics Express. 2014; 5(4):1190–1202. [PubMed: 24761300]
180. Rammohan N, et al. Nanodiamond-Gadolinium(III) Aggregates for Tracking Cancer Growth In Vivo at High Field. Nano Lett. 2016; 16(12):7551–7564. [PubMed: 27960515]
181. Hou W, et al. Nanodiamond–Manganese dual mode MRI contrast agents for enhanced liver tumor detection. Nanomedicine: Nanotechnology, Biology and Medicine. 2017; 13(3):783–793.
182. Waddington DEJ, et al. Nanodiamond-enhanced MRI via in situ hyperpolarization. Nature Communications. 2017; 8:15118.
183. Mkandawire M, et al. Selective targeting of green fluorescent nanodiamond conjugates to mitochondria in HeLa cells. Journal of Biophotonics. 2009; 2(10):596–606. [PubMed: 19504515]
184. Fox K, et al. Nanodiamond-polycaprolactone composite: A new material for tissue engineering with sub-dermal imaging capabilities. Materials Letters. 2016; 185:185–188.
185. Khanal D, et al. Nanotoxicity of nanodiamond in two and three dimensional liver models. International Journal of Nanotechnology. 2017; 14(1–6):133–154.
186. Shenderova O, et al. Commercial quantities of ultrasmall fluorescent nanodiamonds containing color centers. 2017
187. Zhang T, et al. Targeted nanodiamonds as phenotype-specific photoacoustic contrast agents for breast cancer. Nanomedicine (Lond). 2015; 10(4):573–87. [PubMed: 25723091]
188. Jimenez CM, et al. Nanodiamond-PMO for two-photon PDT and drug delivery. Journal of Materials Chemistry B. 2016; 4(35):5803–5808.

189. Bendali A, et al. Synthetic 3D diamond-based electrodes for flexible retinal neuroprostheses: Model, production and in vivo biocompatibility. Biomaterials. 2015; 67:73–83. [PubMed: 26210174]

190. Hadjinicolaou AE, et al. Electrical stimulation of retinal ganglion cells with diamond and the development of an all diamond retinal prosthesis. Biomaterials. 2012; 33(24):5812–20. [PubMed: 22613134]

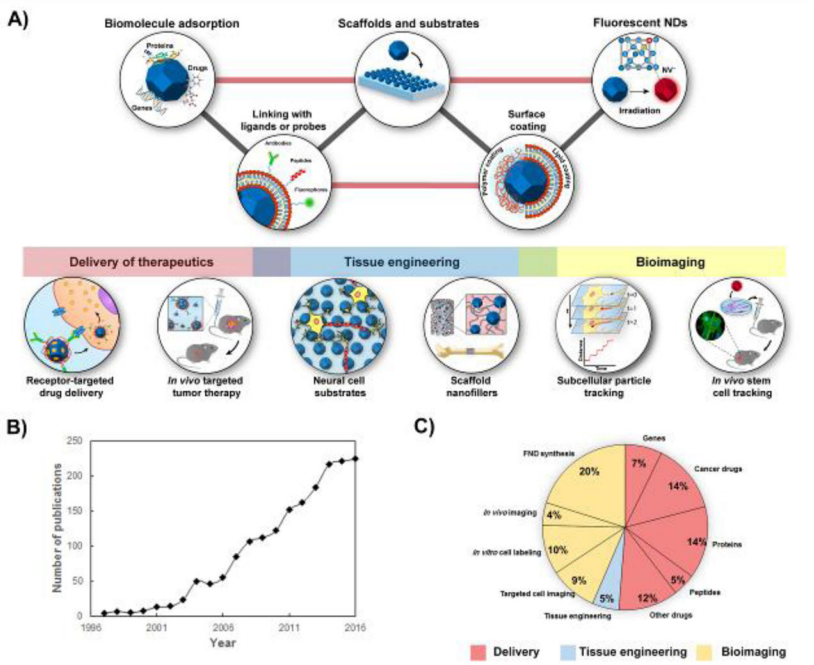

Figure 1.

A) Schematic representing the major fields of research involving the use of NDs. Three major areas can be identified including drug delivery of biomolecules and genes, tissue engineering, and bioimaging. **B)** Graph showing the increase in the number of nanodiamond publications per year over the last twenty years (1990–2017). **C)** Pie chart displaying the percentage of publications (n=248 publications total) since the year 2000 in which NDs were used as nanomaterials for biomolecule delivery, bioimaging and tissue engineering applications. Each area of research has been categorized according to the type of biomolecule delivered or the specific bioimaging application. Data for B and C are obtained from Web of Science, December 2016.

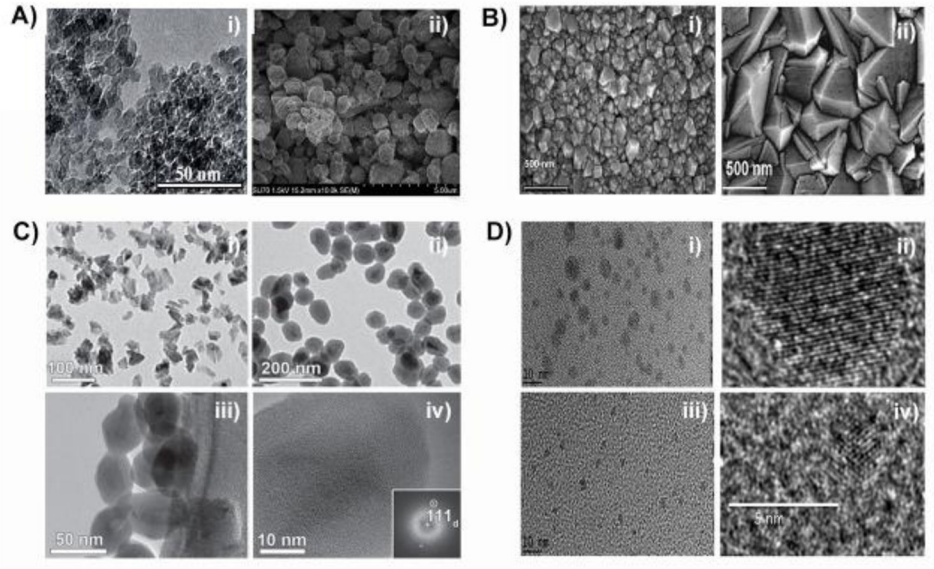

Figure 2.

Differences in size distribution and morphology of nanodiamond particles obtained by different synthesis techniques. **A)** Transmission electron microscopy (TEM) and scanning electron microscopy (SEM) images reveal the differences in morphology of detonation nanodiamond (DND) depending on the synthesis technique. **i)** TEM image of single digit DND. Scale bar represents 50 nm. **ii)** SEM images of micro-dispersed sintered DNDs. Grid unit represents 5 nm [39]. **B)** SEM images of ND films deposited by hot filament CVD with CH_4 and H_2 gas. **i)** Deposition duration of 10 minutes produced a film with a grain size of 50–70 nm and thickness of 100 nm. Scale bar represents 500 nm. **ii)** Deposition duration of 60 minutes, produced a film with 300 nm grain size and thickness of 700 nm. Scale bar represents 500 nm [40]. **C)** TEM images of high-pressure high-temperature (HPHT) nanodiamonds **i)** without surface modification. Scale bar represents 100 nm and **ii)** aminosilica-coated HPHT NDs, scale bar represents 200 nm. **iii)** and **iv)** Higher magnification TEM images of the amino-modified silica-coated HPHT NDs displaying a uniform silane layer on the surface. Scale bar represents 50 nm for image iii and 10 nm for image iv [41]. **D)** TEM images of NDs obtained using ultrafast laser irradiation of ethanol. **i)** and **ii)** TEM images with different magnifications obtained from samples grown with a laser energy of 180 μJ. **iii)** and **iv)** TEM images with different magnifications displaying smaller size and more uniformity for the NDs grown with a laser energy of 620 μJ. Scale bars represents 10 nm for the images **i)** and **iii)** and 5 nm for the images **ii** and **iv)** [42].

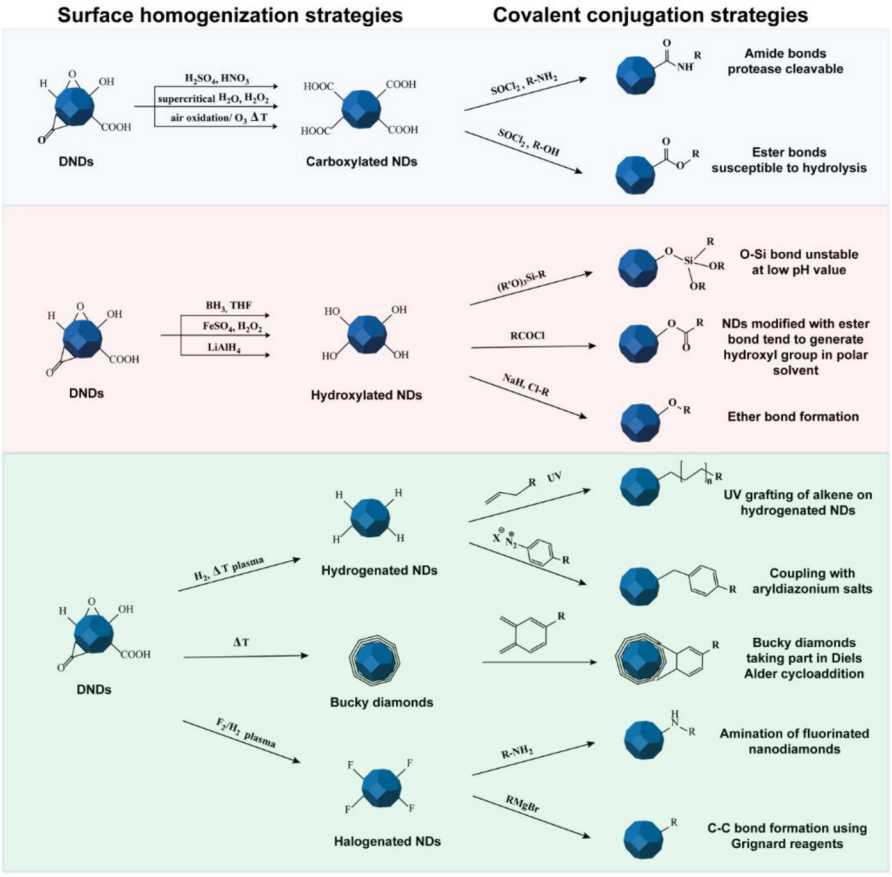

Figure 3.

Chemical modification of denotation nanodiamonds (DNDs). DNDs initially display a heterogeneous distribution of oxygen-related functional groups deriving from the step of purification and oxidation with strong acids. The first step is the surface homogenization which creates a uniform distribution of functional groups on the surfaces of the DNDs. Possible strategies include the introduction of carboxyl or hydroxyl groups to form hydrophilic NDs. Alternative routes of surface homogenization include hydrogenation, halogenation, and temperature annealing. The latter technique is used to form an intermediate carbon phase known as bucky-diamonds, which have a fullerene-like shell consisting of multiple layers of sp^2 carbon. The second step involves a variety of other chemical reactions which are dictated by the reactivity of the functional groups introduced on the NDs' surface. Each of the modification proposed can be potentially used for the covalent conjugation of biomolecules with endless possibilities in drug delivery, tissue engineering, and bioimaging applications.

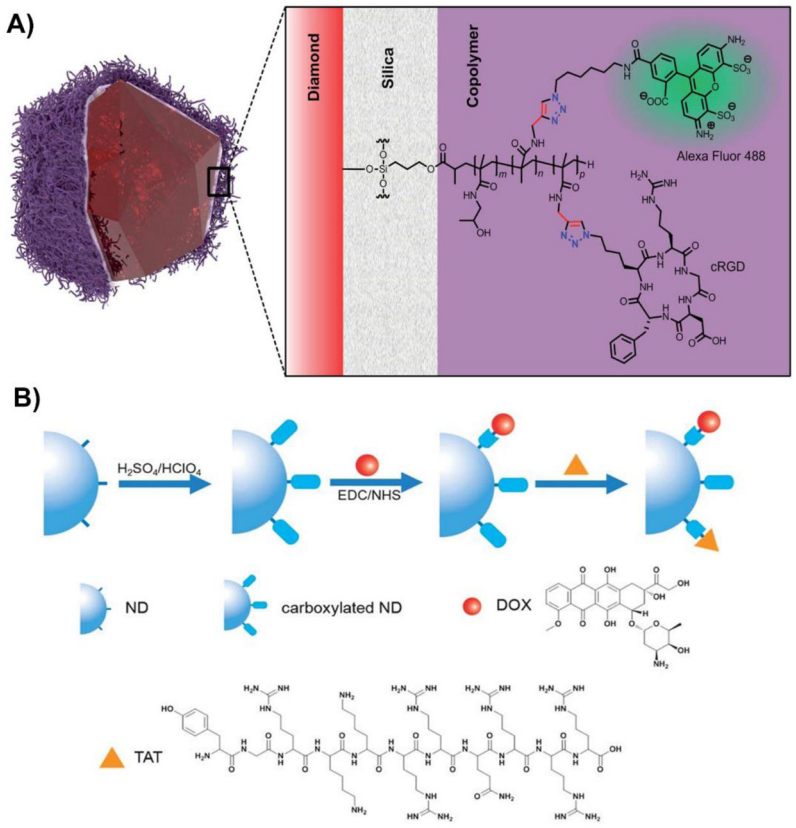

Figure 4.

Strategies for covalently conjugating peptides to the surfaces of NDs for cell targeting. **A)** Schematic representing silica-coated fluorescent NDs containing a copolymer outer shell of methacrylamide that displays the cyclic RGD peptide. The surface of hydroxylated NDs has been modified with a layer of silica which is used as grafting spacer for a synthetic biocompatible copolymer. The polymer coating has been functionalized with the targeting peptide cRGD and with Alexa Fluor 488 as the secondary fluorescent probe. Both molecules have been covalently conjugated using click chemistry [114]. **B)** An example of an alternative strategy for targeted drug delivery using carboxylated NDs obtained after a step of oxidation in strong acids. The activation of the carboxylic groups with NHS/EDC enables the covalent conjugation with both the drug (Dox) and the cell-penetrating peptide TAT on the surface of NDs [117].

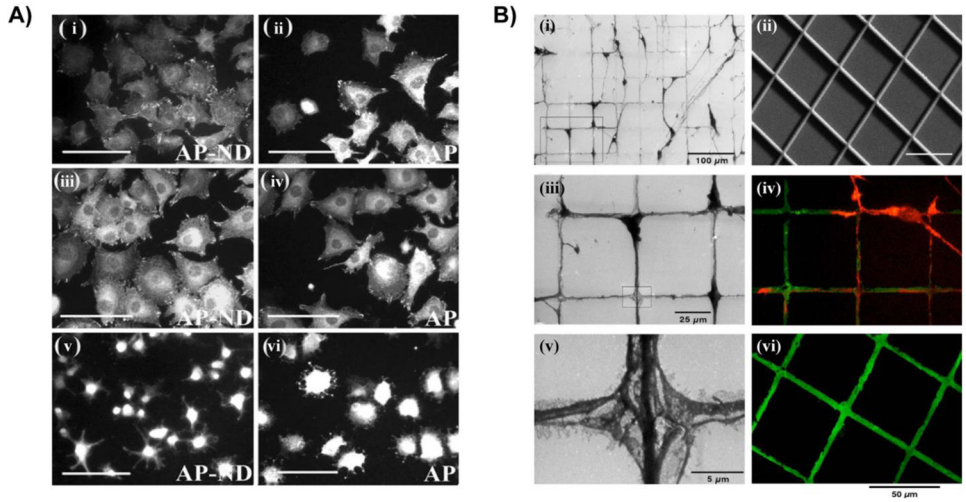

Figure 5.

Surface coating techniques for depositing nanodiamonds (NDs) onto substrates in thin films that improve cell-adhesive properties of conventional cell substrates and enable precise spatial control over cell attachment and proliferation. **A)** Vinculin staining of human osteoblast-like MG-63 cells revealing cell morphology and focal adhesions after 2 hours of culture on electrodeposited layers of apatite (AP) with oxidized detonation NDs. (i–ii) Images indicate the cell seeded on samples coated with serum (i–ii), with fibronectin (iii–iv) and without any protein adsorbed (v–vi). Scale bars = 100 μm [135]. **B)** Laminin was directly microprinted onto hydrophilic ND monolayers which supported the spatially-controlled adhesion and growth of dissociated murine cortical neurons. (i, iii, v) environmental scanning electron microscopy (ESEM) images of cortical neuron culture growing on micropatterned laminin on hydrophilic ND substrate. (ii) SEM image of micropatterned laminin on ND surface. Scale bar represents 50 μm. (iii) An enlarged view of the region indicated by the highlighted region is displayed below in (v) which displays the ordered neurite extension and outgrowth across the bare ND substrate at the intersection of the pattern. (iv, vi) Fluorescent images displaying F-actin staining (green) of ordered neurite outgrowth on laminin-coated diamond surfaces (red) after (iv) 48 hours of culture and after (vi) 7 days [146].

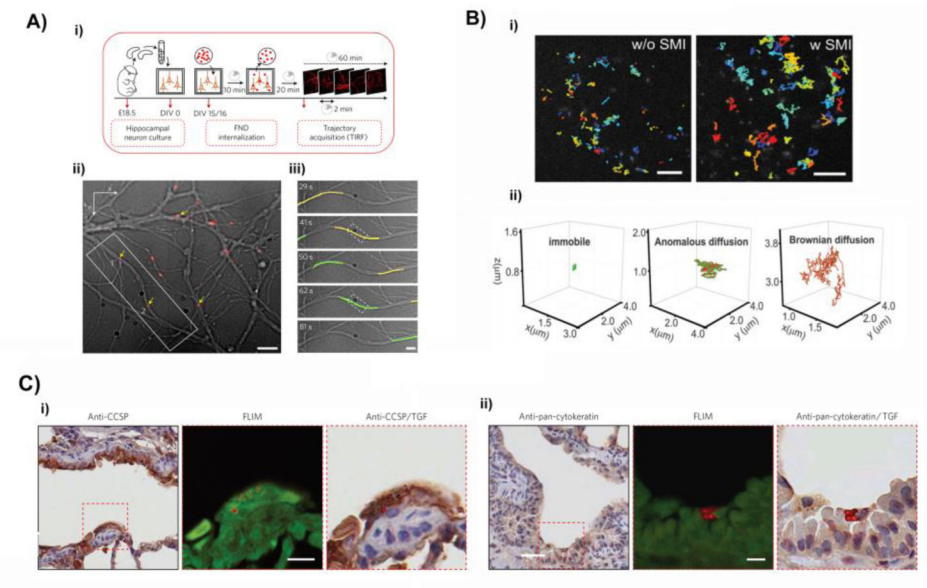

Figure 6.

Uses of fluorescent NDs as bioimaging probes. **A)** Single particle tracking of FNDs to evaluate intraneuronal transport. i) Schematic and timeline of the experimental setup beginning with the expansion of hippocampal neuron cells, followed by fluorescent labeling of cells by internalization of FNDs, and video acquisition of FNDs inside cells by pseudo-total internal reflection fluorescence video microscopy (pseudo-TIRF). ii) Bright-field image overlayed with the fluorescent channel to display the localization of FNDs (indicated in red) throughout a neuronal branch at a single time point. The yellow arrows identify four FNDs moving through dendrites. The FNDs labeled 1 and 2 were localized in the same branch and were being transported towards the soma of the neuron (not visible in this image). The scale bar represents 5 μm. iii) An expanded view of the two FNDs labeled in part ii), displaying the trajectory of each particle (indicated by the yellow and green markings) over 10 seconds at several time periods. The scale bar represents 1 μm [168]. **B)** Single-particle tracking (SPT) of proteins in transmembrane signaling. i) Single-particle trajectories of FND-labeled TGF-β in human adenocarcinoma cells, both unmodified (w/o SMI) and with the treatment of a small molecule kinase inhibitor (w/SMI). ii) Three distinct diffusion states were identified when the FND-labeled protein was tracked in adenocarcinoma cells [169]. **C)** Investigation of stem cell tracking *in vivo* using fluorescent NDs. i) Immunostaining of club cell markers (CCSP) and ii) epithelial markers (pan-cytokeratin) in lung tissue sections obtained from naphthalene-injured mice on day 7 after being injected intravenously with lung progenitor stem cells (LSCs) labeled with fluorescent NDs (FNDs). In the middle, fluorescence lifetime images (FLIM) of FNDs-labelled LSCs and corresponding enlarged merged images of immunostaining and TGF images showing the presence of LSCs in the epithelial region of the lung. The scale bar represents 10 μm [164].

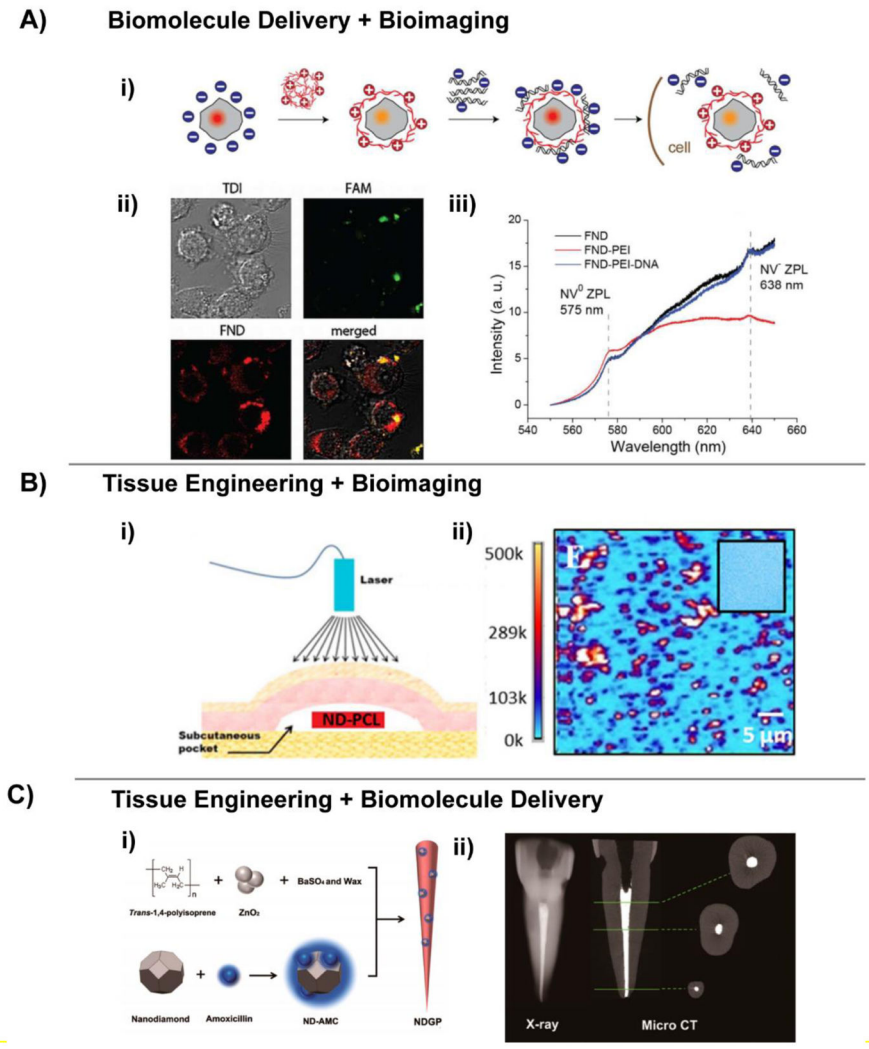

Figure 7.

Recent studies displaying the applications of NDs as a multimodal platform for biomolecule delivery, tissue engineering, and bioimaging. **A)** FNDs used both as a gene delivery platform and bioimaging platform to enable real-time imaging of DNA transfection in live cells. **i)** Schematic showing the formation of an electrostatic complex between the FND-PEI-DNA on the surface of the nanoparticles followed by the release of DNA and internalization in the cell. FND display a change in the emission colors upon interaction with PEI and DNA. **ii)** Images displaying the internalization of DNA released from the FND-PEI-DNA complex in IC-21 macrophages after 120 minutes. DNA was labeled with fluorescein (FAM) before formation of the complex with PEI. Red luminescence represent the NV centers in FNDs. **iii)** Photoluminescence (PL) spectra of oxidized FND and the complexes with only PEI and PEI+DNA obtained in water after an excitation at 514 nm. The FND-PEI complex showed a significant reduction in the NV^- luminescence compared to oxidized FNDs. Additionally, upon complexation with negatively charged DNA the luminescence increases again to the original value of oxidized FNDs [174]. **B)** Composite scaffolds formed with FNDs and polycaprolactone (PCL) were implanted subcutaneously in pigs, and the tracking abilities of

FNDs were demonstrated *in vivo*. **i)** Schematic of the custom confocal microscopy setup to image the FND-PCL scaffold *in vivo*. **ii)** Fluorescent heat map of the scaffold material. The regions in red indicate the presence of the FNDs with notable aggregation [184]. **C)** ND-modified gutta-percha for enhanced root canal therapy. **i)** Schematic showing the synthesis of gutta-percha and ND complexes. Carboxylated NDs were non-covalently linked with amoxicillin, and then mixed with gutta-percha to produce NDGP. **ii)** X-ray and micro-CT scan of a human patient-derived central incisor that has been obturated with NDGP. Middle, coronal, and apical cross sections were examined and reported to contain no voids after filling with NDGP [128].

Table 1

Summary of the available strategies for the synthesis of NDs

Synthesis technique	Average size	Morphology	Surface chemistry	Advantages	Limitations
Detonation synthesis	4–5 nm	Truncated octahedral morphology	Heterogeneous with sp^2 hybridized carbon and other metal impurities. Oxygen functional groups (hydroxyl, carboxyl, carbonyl, epoxy)	Industrial scale production	Formation of aggregates (~ 200 nm or larger) Different steps of purification are required High costs due to the process of purification Hazardous and polluting technology
Chemical vapor deposition (CVD)	5–100 nm	NDs films	Hydrogenated surface	Absence of metal impurities Useful for fabricating films	Strategy limited to the production of films High production costs
High-pressure and high-temperature (HPHT)	>20 nm	NDs with sharply faceted outer surfaces	Absence of sp^2 defects on the surface	Uniform size Higher nitrogen content useful for imaging applications	High production costs
Light hydro-dynamic pulse synthesis (LHDP)	4–5 nm or 250–300 nm	NDs with similar morphology of DNDs	Controlled surface chemistry	Environmentally friendly technology Control over the size High purity NDs production with high homogeneity	Early technology with limited transition to mass production

J Control Release. Author manuscript; available in PMC 2018 September 10.

Table 2

Influence of surface modification on the NDs' cytotoxicity

Type of NDs and average size	Surface modification	Type of cells	Range of concentration tested	Biological response	Ref
DNDs 100 nm	-COOH	A549 (lung cancer cells) and 3T3-L1 embryonic fibroblasts	100 μg/mL	No influence of NDs on the cell growth, and adipogenic differentiation	[83]
Syndia® SYP 0–0.02: ND-20 nm and Syndia® SYP 0–0.1: ND-100 nm).	-COOH	HepG2 and Hep3B (liver), Caki-1 and Hek-293 (kidney), HT29 (intestine) and A549 (lung)	250–500 μg/mL	No sign of cytotoxicity or genotoxic effect	[77]
DNDs 4–5 nm	-COOH	Mouse embryonic stem cell	2.5–100 μg/mL	Higher genotoxicity in carboxylated NDs compared to pristine NDs	[78]
Fluorescent NDs 120 nm	-COOH	Mouse P19 ECS and human NT2/D1	0.1–50 μg/mL	No sign of apoptosis or cytotoxicity	[84]
NDs 270 nm	-COOH	hASCs	1.5 μg/mL	No effect on morphology, differentiation and no sign of inflammation	[85]
HPHT NDs 100–120 nm	$-NH_2$	HepG2 and HeLa	1–1000 μg/mL	No influence in metabolic activity or apoptosis	[86]
DNDs 4 nm	$-NH_2$, -COOH and -OH	HEK cells	10–200 μg/mL	Cytotoxic effect is dependent on the dose. Cytotoxicity decreased in this order: $NH_2 \gg OH > COOH$ at high concentration	[79]
DNDs 5 and 100 nm	-SH	Human A549 (lung cancer cell)	0.1–50 μg/mL	No cytotoxic effect due to the thiol groups	[87]
DNDs -	Polymer composite PANI-NDs	HEK cells	0.1–10 μg/mL	Cytotoxic effect of the PANI coating at concentration of 10 μg/mL	[81]
DNDs 28–32 nm	Surface conjugation with ODA	Murine osteoblasts	100 μg/mL	No cytotoxic effect	[82]
DNDs 4–5	Coating with PG (DNDs-PG)	U937 Macrophages	50–200 μg/mL	No cytotoxic effect on macrophages	[88]

Abbreviations: Human adipose mesenchymal stem cell (hASCs), embryonal carcinoma stem cell (ECS), Ntera -2 D1 cell (NT2/D1), Human alveolar epithelial cells (A549), embryonic kidney cells, polyaniline (PANI), octadecylamine (ODA), PG Hyberbranched polyglycerol.